INVESTIGATION AND PERFORMANCE ANALYSIS OF NANOSCALE COMMUNICATION NETWORK FOR BIOMEDICAL APPLICATION

By

Farhana Ahmed Liza
16121018
Mahmudul Hasan
16121058
Nusrat Islam
16121089
Tanmoy Paul
16121151

A thesis submitted to the Department of Electrical and Electronic Engineering in partial fulfillment of the requirements for the degree of
Bachelor of Science in Electrical and Electronic Engineering

Electrical and Electronic Engineering
BRAC University
August 2019

Declaration

It is hereby declared that

1. The thesis submitted is our own original work while completing degree at BRAC University.
2. The thesis does not contain material previously published or written by a third party, except where this is appropriately cited through full and accurate referencing.
3. The thesis does not contain material which has been accepted, or submitted, for any other degree or diploma at a university or other institution.
4. We have acknowledged all main sources of help.

Student's Full Name & Signature:

Farhana Ahmed Liza 16121018	**Mahmudul Hasan** 16121058
Nusrat Islam 16121089	**Tanmoy Paul** 16121151

Approval

The thesis titled "Investigation and Performance Analysis of Nanoscale Communication Network for Biomedical Application" submitted by

1. Farhana Ahmed Liza (16121018)
2. Mahmudul Hasan (16121058)
3. Nusrat Islam (16121089)
4. Tanmoy Paul (16121151)

of Summer, 2019 has been accepted as satisfactory in partial fulfillment of the requirement for the degree of Bachelor of Science in Electrical and Electronic Engineering on 29th of August.

Examining Committee:

Supervisor:
(Member)

_____
Saifur Rahman Sabuj, PhD
Assistant Professor, Department of Electrical and Electronic Engineering
BRAC University

Program Coordinator:
(Member)

_____
Saifur Rahman Sabuj, PhD
Assistant Professor, Department of Electrical and Electronic Engineering
BRAC University

Departmental Head:
(Chair)

_____
Shahidul Islam Khan, PhD
Professor and Chairperson, Department of Electrical and Electronic Engineering
BRAC University

Abstract

Biomedical application consists of the transmission of information inside the human body using nanoscale communication network. This transmission is affected by a number of factors. In this thesis, our goal was to investigate the behavior of different factors inside the human body. We have used the Debye Relaxation model to investigate the effect of polarization inside the human body, the effect of relative permittivity with respect to terahertz band in different tissues. After that, we have investigated the parameters of path loss, namely spreading loss, absorption loss and scattering loss. Finally, we have observed the behavior of conductivity inside the human about how fast it can receive a signal without being attenuated from different skin perspectives. With the advancement of small-sized-plasmonic signal sources, antennas, and detectors, wireless communications among intrabody nanodevices will be empowered at terahertz band (0.1–10 THz). This outcome motivates real-time monitoring of both medical test parameters, biological and chemical substances inside the human body are yearning that could facilitate pathology control and ensure better diagnostic and treatment effectiveness. Variegated characteristics like polarization, relative permittivity, path loss, conductivity, molecular absorption and outage probability of Terahertz (THz) band impact every fundamental communication system for the exchange of data between nanodevices. The complete pathloss is calculated by the combined impact of propagating wave spread, molecular absorption from human tissues, as well as scattering from both tiny and large body particles. Numerical results show that, skin (dermis and epidermis) has the minimum pathloss and that makes it better choice for nanodevice implantation. The outage probability also shows that it is possible to establish an intrabody communication network in human body.

Keywords: Nanoscale Communication, Biomedical, Pathloss, Terahertz Band, Outage Probability.

Dedication

DEDICATED TO OUR PARENTS

Acknowledgement

At first, we would like to convey our best gratitude to almighty Allah for His kindness and blessing. Without His will it would not have been possible for us to finish this thesis paper which we consider to be our one of the most important learning experiences of our undergraduate life.

We are forever indebted to our supervisor Saifur Rahman Sabuj, PhD, Assistant Professor, Department of Electrical and Electronic Engineering, BRAC University, for providing us with an extraordinary opportunity to work in the arena of nanoscale communication. We consider ourselves very lucky to have got his tireless support and inspiring guidance during the period of research. Next, we would like to express our heartfelt appreciation to all the faculties and staffs of Electrical and Electronic Engineering Department of BRAC University for their unconditional assistance in our hour of need.

At last we would like to thank our parents for always standing by us. It is their care, support and sacrifice that has encouraged us to come this far. We are very much thankful for everything they have done for us.

Table of Contents

List of Tables

List of Figures

List of Acronyms

IoNT	Internet of Nano-Things
BANN	Body Area Nano Networks
EM	Electromagnetic
THz	Terahertz
SNR	Signal-to-Noise Ratio
SDN	Software Defined Network
NFV	Network Function Virtualization
WBAN	Wireless Body Area Network
TE	Transverse Electric
TM	Transverse Magnetic
dB	Decibel
WCN	Wireless Communication Network
GHz	Gigahertz
Tbps	Terabit Per Second
NEP	Noise Equivalent Power
SDP	Shortest Distance Point
WPAN	Wireless Personal Area Network
MN	Master Node

List of Symbols

L_{spr}(f)	Spreading loss
L_{abs}(f)	Molecular absorption loss
L_{sca} (f)	Scattering loss
λ_r	Effective wavelength
n'	Real part of tissue refractive index
n''	Imaginary parts of tissue refractive index
D	Directivity
Ω_A	Solid angle of Gaussian beam
η	Wave impedance in human tissue medium
$\Delta\theta$	Gaussian beam of width
σ_{abs}	Molecular absorption cross section
σ_g	Geometric cross section
ρ_v	Concentration of particles
I_{sca}	Intensity
K	Signal incident radiation factor.
t_{skin}	Thickness of skin
t_{fat}	Thickness of fat
t_{blood}	Thickness of blood
d_{min}	Minimum distance

P_o	Transmission power
δ_c	Multiplication of all antennas gain
P_N	Noise power
K_{sd}	Complex Gaussian random variable with unit variance
β_0	Speed of transmission
δ_{c0}	Channel gain
T_0	Required transmission rate
P_{out}	Outage probability
ε_∞	High frequency level permittivity
ε_1	Permittivity of the medium 1
ε_2	Permittivity of the medium 2
τ_1	Relaxation time for medium 1
τ_2	Relaxation time for medium 2

Chapter 1

Internet of Nano Things

1.1 Introduction to Nanoscale Communication

In the world of biomedical engineering, a vital part is played by the progression in nanotechnology to help boost the standard of the physical condition and the average life expectancy of people, especially because of its benefits of miniature size, bio-stability and the harmlessness on living tissues. Nanotechnology helps in diminishing the extent of the nano devices providing it with new functionalities according to the needs. The suitability of the nano devices in biomedical applications has been expanding rapidly due to the emergence of the nano-materials with astounding properties. Some basic applications may include medicate conveyance and consistent health observation [1].

Nano-communication is the trading of data based on any connected or remote link of the network of nanomachines known as nano-network. An independent nanodevice is exceptionally compelled by finite vitality, processing and the scale of communication, for which a nano-network is developed. A nano-network grows the potentiality of a solo nanodevice by giving an approach to collaborating and sharing data. The vast applications of nano-networks include tissue regenerations, surgical operations, diagnostics, drug delivery etcetera. As such, the detection of tumor and the drug delivery system can be made exact and confined with the help of Internet of Nano-Things (IoNT). The Internet of Nano-Things (IoNT) can be represented as a network model empowered when the nano-network interface with an internet portal by wirelessly covering the data to an external gadget [2].

A standout amongst the most encouraging implementations of nano-networks is their utilization as Body Area Nano Networks (BANN); that includes streaming interrelated nano devices into the circulatory system, announcing data to some authority externally (for

example specialists) or data preparing frameworks. In any case, the structure, usage and organization of nano-networks in a living natural condition presents considerable issues, which must be survived; thus displaying challenges in various research fields, for example, signal propagation, reception apparatuses, and data innovation, in particular. The incredibly high electromagnetic (EM) frequencies necessary for correspondence amidst nnodevices in addition to the specific direct necessities in organic tissues (amazingly high way misfortune and atomic ingestion clamor values) limit signal spread. A conceivable methodology comprises of improving transmission power so as to effectively give/get information. Be that as it may, because of the small size of nanodevices, their accessible energy is profoundly restricted. Under these conditions, an exchange off between the two concerns (transmission control and devoured energy) must be examined and measured. Shockingly, concurring as far as we could possibly know, few examinations in writing tackle this issue. It must be ensuring to appropriately supply the sufficient power for which more exertion must be committed to building up a sensible vitality model [3].

We have another form of communication known as molecular communication, which other than transmitting the information in the form of electrons or electromagnetic waves, uses molecules where the information is coded to and decoded from. Molecular communication takes place within a small distance between nanomachines. Every process in this world occurs in a systematic manner which if further analyzed makes it easier to work on. As such, in biological systems, the molecular communication also has systems and modes of different variation, and it can be set up to a generalized model for a better understanding of the structure standards [12].

All the elements of a molecular communication are consisted of molecules. Such as, ions act as information molecules; sender and receiver nanomachines send and detect those ions respectively, molecular motors as transport molecule, actin filament as guide molecules. To

let the transport molecule to convey the information molecule, vesicles are used as interface molecules. It should also be considered that large amount of noise (which determines the degree of randomness of molecular communication) is produced as the environment used to transit the information molecules is either aqueous or air. This noise can be developed for a number of reasons, one of which can be the contact of force and energy in the environment, with the molecular elements. Some molecules and machines in the environment are not involved in the molecular communication. Such as, water molecules, nanomachines that preserve the chemical concentration, and energy molecules to uphold the nanomachines. All these contribute in the production of noise.

During molecular communication, the molecules carry out their tasks in four stages: the sender nanomachine encodes the information into an information molecule (encoding), conveying the information molecule into the environment (sending), transmission of the information molecule through the environment (propagation), the information molecule is accepted by the information molecule which is decoded it into a chemical processing (receiving).

- **Encoding:** The sender nanomachine converts and encodes the data into an information molecule which can be recognized by the receiver nanomachine. The receiver nanomachine can just receive a particular quantity of information depending on the quantity of the arrangements of the receiver nanomachine. For example, if a receiver nanomachine comprises of two arrangements then it can comprehend one bit at a time. So, the sender nanomachine has to encode the information accordingly. If the sender nanomachine transfers information of which the receiver nanomachine does not have data then the sender nanomachine can send arbitrary information molecule which can initiate new functionality in the receiver cells.

- **Sending:** Here the sender nanomachines conveys the information either by unbinding the information molecules from itself or by letting the information molecule to disperse away, by opening a gate. A single sender nanomachine has a restricted communication capacity as it has a constrained measure of energy and information molecule due to its size, so it depends on the environment to provide it with energy and information molecules. Also, a stronger signal can be generated in the environment by using various sender nanomachines.
- **Propagation:** This is the transmission of the information molecule by means of the environment from the sender nanomachine to the receiver nanomachine. The transmission can be either active or passive. In passive transmission, the information molecule binds to a transport molecule which moves using forces in the environment, and this causes slower diffusion for larger molecules. Whereas, in active transmission it requires energy. Here, the effectiveness of transmission can be improved and the time needed for the transmission can be reduced, by giving more power over the development of information molecules. In the time of transmission, the information molecule can be transmitted in an interface molecule to prevent the information molecule from noise in the medium.
- **Receiving:** The information molecule is received by the receiver nanomachine and further decoded into a chemical reaction. The reception can be done in two ways, it can either use a receptor which binds to the specific information molecule, or it can use channels which help the information molecules to flow in without using receptors.

1.2 Review of Previous Work and Observation

For the past few year researchers have been working on the possibilities and the limitations of the nano-networks inside a human body using nanodevices. As such the terahertz in-vivo nano-networks, mac protocol, channel demonstration for wireless body area network have been analyzed and proposed in different papers. In this section, we have talked about some of these works of various authors.

Rui Zhang *et al.* (2017) presented a systematic model of the terahertz (THz) communication channel (0.1 - 10 THz) in their paper. Taking into account the influence of noise on link quality and data rate, the model has been presented for the in-vivo nano-networks. They examined the signal-to-noise ratio (SNR) of the communication channel for multiple power allocation schemes, and the most outrageous reachable data rate is concentrated to examine the capability of THz communication inside a human body. Their studies show that the attainable transmission distance of in-vivo THz nano-networks ought to be controlled to roughly 2 mm most extreme, while the operation band of in-vivo THz nano-networks ought to be constrained to the lower band of the THz band and that the information rate is negatively correlated to the transmission distance [1].

Antonio-Javier Garcia-Sanchez *et al.* (2018) have contributed with a various leveled BANN architecture comprising of two sorts of nano-devices, to be specific, nanonodes and a nanorouter in their paper. In case of communication being established in human hand, as though the negative effect of path loss and the molecular absorption noise on the spread of Electromagnetic propagation in less severe but the nano-devices must be powered through the circulation system and outer ultrasound energy harvesting sources as the minor size of nano-devices and their amazingly restricted vitality putting away capacity limits the data transmission. The outcomes from the inspection and examination of necessary energy

uncovered the exceptional capacity of nanonodes to energize, in this manner empowering one pair of nanonode–nanorouter to convey each 52 min [2].

Akram Galal *et al.* (2018) have presented how the fusion of Software Defined Network (SDN), Network Function Virtualization (NFV) and IoT technologies, can help in Nano-networks' settings, combined with an unified architectural model of Nano-network communication. Thus, they propose a lot of capacities and use cases that can be executed by Nano-devices and talk about the noteworthy difficulties in actualizing these capacities with Nano-technology worldview and the open research issues that should be tended to [3].

Ke Yang *et al.* (2017) have analyzed and introduced the probability distribution signal-to-interference-plus-noise ratio (SINR) for THz communication within different human tissues, for example blood, skin, and fat, and also developed an interference model using TS-OOK as a communication scheme of the THz communication channel inside the human body. They have investigated the mean investigations of SINR under various node densities in the area and the probabilities of transmitting pulses which helped them to assess the performance degradation and thus brought out the result that the interference controls the reachable communication distance to roughly 1 mm [4].

Hadeel Elayan *et al.* (2017) have worked considering the transmitter power, medium path loss, and receiver sensitivity, where both the THz and photonic devices has been taken into account. They have performed the examination of the first system required for directing link budget analysis amidst nano-devices working inside a human body. The general constriction model of intrabody THz also, optical frequency propagation encourages the precise plan and actual deployment of iWNSNs [5].

David B. Smith *et al.* (2015) in their paper have described the working conditions of the wireless body area network both inside and outside the human body, from one body to another, and also the carrier frequencies that may vary between hundreds of MHz to several

GHz; and bandwidth at which the utilization will take place, comprising narrowband and ultra-wideband. Especially two challenging situations for the BAN operation have been described: supervising while in sleep and also where there is an enormous number of co-located BANs, and the ruling of the BAN channel by shadowing with gradually evolving dynamics have been exhibited as the result [6].

Qammer H. Abbasi *et al*. (2017) have introduced an epic idea of cooperative communication for in-vivo nano-network to improve the communication among the nano-devices. For different parameters including relay placement, number of relays, transmit power, bandwidth and carrier frequency, the impact on functionality of the system outage probability is carried out which showed the result that the system outage performance increments by 10-fold in the cooperative network with an extra relay, which demonstrates an incredible potential of utilizing cooperative communication to enhance the presentation of nano-network at terahertz frequencies [7].

Jaeho Lee *et al.* (2018) proposed a new MAC protocol in order to expand the lifetime of the nodes of the Wireless Body Area Network (WBAN), by planning the asymmetrically energy-balanced model among nodes and coordinator to fulfill the increased effectiveness of energy of nodes than coordinator, which in turn stacked the unpreventable intake of energy into the coordinator rather than the nodes. Moreover, the plan additionally gave prioritization to the urgent transmission of data with differentiated Quality of Service (QoS) [8].

P. Kaythry *et al.* (2018) have worked to conquer the energy and reliability issues by analyzing the feasibility and execution of fountain code based raptor code for error correction, whose flexibility in terms of code gain and code rate has been proven advantageous to increase the energy efficiency of WBAN network. Compared to LT code, traditional BCH code and ARQ error control technique, the raptor coded packet transmission is more energy efficient which had been shown in the simulation results [9].

Kazuhiro Tsujimura *et al*. (2018) have chosen the range of 0.1-10 THz impulse response for short range wireless communication of 1-100 cm. They have worked on the issue of the symmetric impulse response of not being able to reach before the line-of-sight (LoS) physically, sit violates causality, whereas the linear phase is supposed to prompt a symmetric impulse response before and after the LoS propagation delay. The examination determines a phase function prompting an impulse response satisfying causality. The legitimacy of the determined model is confirmed with test THz band estimations (up to 2 THz), which show magnificent concurrence with the outcomes anticipated by the hypothesis. Their result show huge varieties in the coherence bandwidth as a function of the center frequency for both the entire THz band and its sub-bands [10].

Apostolos K. Vavouris *et al.* (2019) have presented the productive utilization of a novel modulation scheme in body-centric terahertz (THz) nano-networks, which is a blend of the time-spread On-Off keying (TS–OOK) and the pulse position modulation (PPM) furthermore contrasting with another current strategies as TS–OOK, at a lesser value to the data rate presents lower energy consumption. Finally, they have presented the results of their analysis and simulation so as to contrast the new plan and the current TS–OOK, and that the plan proposed could be adequately used to relieve the effect of the particular sort of noise in THz body-centric communication, therefore prompting better error performance [11].

1.3 Objectives

- To investigate the behavior of different factors inside the human body for Terahertz (THz) band in biomedical applications.
- To study of polarization, relative permittivity, path loss and conductivity.
- To investigate the outage probability of Terahertz (THz) band in biomedical sector.
- To review intra-body pathloss in human hand scenario.

1.4 Organization of the Thesis

We included four chapters in our thesis which are:

Chapter-1 is the introductory chapter. Here we have discussed about some basics of biomedical applications, described about the Internet of Nano-Things (IoNT), talked about the Body Area Nano Networks (BANN) and the molecular communication. After that we have done a literature review on the previous works followed by the objective of our thesis.

Chapter-2 presents eight parts. In the first four parts we have investigated the effect of parallel and perpendicular polarization inside the human body and discussed the polarization that happens due to transverse electric and transverse magnetic waves. Then path loss parameters have been observed considering the effect of only spreading loss and we have observed molecular absorption loss and the conductivity of different human skin layers. We have shown how different parameters amounted to path loss in terahertz communication and the impact of these propagation losses in human body. We have explained these through human hand scenario. Finally, we have employed analysis of outage probability.

Chapter-3 contains the analysis of the graphs using MATLAB. There we have tried to compare the path loss of different human tissues as we have varied the frequency and distance.

Chapter-4 presents our concluding remarks and mentions about our limitations as well as our plan to proceed with this research work further in the future.

Chapter 2

Behavior of Different Factors inside the Human Body

2.1 Parallel and Perpendicular Polarization

When waves propagate through the similar waveguide medium like different kinds of cables and void channel, TE and TM waves are produced. Both TE and TM waves have electric field (E) and magnetic field (H) component. Here, in the Figure 2.1, the direction of wave is assumed to be in the z direction and other two directions are the TM and TM wave components. For the determination of electric and magnetic field of transverse electric and magnetic wave, we utilize the Maxwell's curl equation [13].

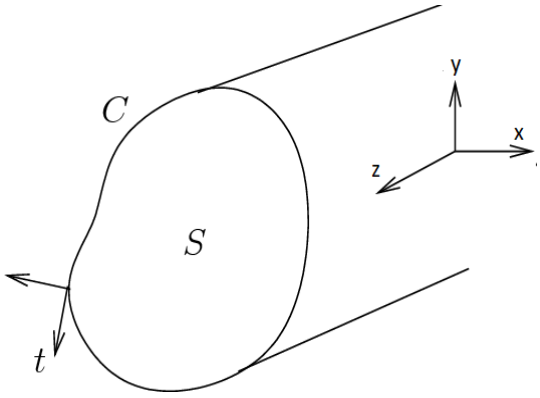

Figure 2.1: Concept of TE and TM Wave

At TE: Electric component at z direction, $E_z = 0$ and magnetic component at z direction, $H_z \neq 0$.

At TM: $E_z \neq 0$ and $H_z = 0$.

So, the variations between their electric field and magnetic are the main dissimilarity between them. Now, TE as well as TM waves results in polarization. Transverse electric wave yields to perpendicular polarization and transverse magnetic wave yields in parallel polarization.

Those two phenomenon are described by the law of reflection as both of them have same angle of incidence and reflection.

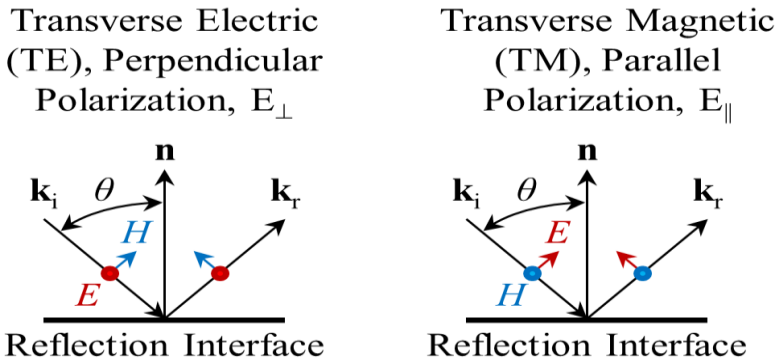

Figure 2.2: Perpendicular Polarization and Parallel Polarization

Here, figure shows the relationship between TE and TM waves in terms of reflection perspective where, k_i is the incident ray and k_r is the reflected ray, n is the normal line and electric and magnetic field of TE and TM waves are denoted by E and H which are transverse element of those [13].

So far we have discussed about the TE and TM waves and the polarization because of these. Now, this leads to the angle of polarization which can also be called as the Brewster's angle. It is the Brewster's angle, known as the angle of incidence, at which the polarized wave flawlessly propagates through the lucid surface. The Brewster's angle remains amidst the polarized and faintly polarized.

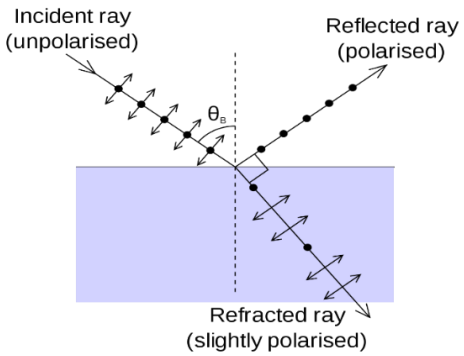

Figure 2.3: The Brewster's Angle

Now, to find the values of power reflection coefficient versus angle of incidence, we used Debye Relaxation model where dielectric response in frequency domain of various tissues are considered [5]. The Double Debye equation [5] which gives us complex permittivity as –

$$\varepsilon = \varepsilon_{\infty} + \sum_{j=1}^{n} \frac{\Delta\varepsilon}{1+j\omega\tau j} \quad \text{..... (2.1)}$$

$$\varepsilon = \varepsilon_{\infty} + \frac{\varepsilon 1 - \varepsilon 2}{1+j\omega\tau 1} + \frac{\varepsilon 2 - \varepsilon_{\infty}}{1+j\omega\tau 2} \quad \text{..... (2.2)}$$

Equation (2.2) is rationalized. Here, ε_{∞} is the permittivity value at very high frequency, ε_1 and ε_2 is the permittivity of different mediums and τ_1 and τ_2 is the relaxation time associated with the relaxation process.

Equation (2.2) is divided into two parts as real part and as imaginary parts which gives us -

$$\varepsilon' = \varepsilon_{\infty} + \frac{\varepsilon 1 - \varepsilon 2}{1+(\omega\tau 1)^2} + \frac{\varepsilon 2 - \varepsilon_{\infty}}{1+(j\omega\tau 2)^2} \quad \text{.....(2.3)}$$

and

$$\varepsilon'' = \frac{(\varepsilon 1 - \varepsilon 2)(\omega\tau 1)}{1+(\omega\tau 1)^2} + \frac{(\varepsilon 2 - \varepsilon_{\infty})(\omega\tau 1)}{1+(j\omega\tau 2)^2} \quad \text{.....(2.4)}$$

Equation (2.3) is the real part of equation (2.2) and Equation (2.4) is the imaginary part of equation (2.2).

we can write from (2.3) and (2.4) that,

$$A = \frac{(\varepsilon 1 - \varepsilon 2)(\omega\tau 1)}{1+(\omega\tau 1)^2} \quad \text{.....(2.5)}$$

$$B = \frac{(\varepsilon 2 - \varepsilon_{\infty})(\omega\tau 1)}{1+(j\omega\tau 2)^2} \quad \text{.....(2.6)}$$

$$C = \varepsilon_{\infty} + \frac{\varepsilon 1 - \varepsilon 2}{1+(\omega\tau 1)^2} \quad \text{.....(2.7)}$$

$$D = \frac{\varepsilon 2 - \varepsilon_{\infty}}{1+(j\omega\tau 2)^2} \quad \text{.....(2.8)}$$

We can also write that,

$E = \cos(\theta)$ …….(2.9)

$F = \sin(\theta)$ …….(2.10)

where, $\omega = 2*\pi*f$. Here, ω is the angular frequency [14].

$\varepsilon_{imaginary} = A + B$ ……..…….……(2.11)

$\varepsilon_{real} = C + D$…….…….....(2.12)

$\varepsilon_{complex} = (\varepsilon_{real} - j * \varepsilon_{imaginary})$ ……......(2.13)

$\varepsilon_{mag} = abs(\varepsilon_{complex})$……(2.14)

Now, parallel reflection– $\frac{Y}{Z}$ and perpendicular reflection– $\frac{Y1}{Z1}$

where, $Y = abs((-B*E) + \sqrt{(B - F^2)})$…….(2.15)

$Z = abs((B*E) + \sqrt{(B - F^2)})$…….(2.16)

and

$Y1 = abs(E - \sqrt{(B - F^2)})$ ……...…….(2.17)

$Z1 = abs(E + \sqrt{(B - F^2)})$ ……..…….(2.18)

∴ Parallel power reflection coefficient = (parallel reflection)^{2}and Perpendicular power reflection coefficient = (perpendicular reflection)^2

We observed the simulation result of parallel and perpendicular power reflection coefficient in terms of blood, plasma, water, dermis and epidermis.

2.2 Permittivity and Relative Permittivity

Permittivity or usually called absolute permittivity is defined as – when in different mediums electric field is configured, capacitance is also experienced due to it. It also describes the generation of one electric charge in different types of medium. It is denoted by ε (epsilon) and its SI unit is F/m (Farad per meter). In the polarization of the medium, permittivity stores electric field in it. Now, relative permittivity is responsible for the reduction in electric field and is denoted by ε_r. Relative permittivity is the dimensionless number and it also complex natured. Relative permittivity is also known as the dielectric constant and denoted by k. We can define relative permittivity as –

$\varepsilon_r = \frac{\varepsilon}{\varepsilon 0}$, here the permittivity of the medium is ε.

Now, complex permittivity can be found from equation (2.2)

$$\varepsilon = \varepsilon_{\infty} + \frac{\varepsilon 1 - \varepsilon 2}{1 + j\omega\tau 1} + \frac{\varepsilon 2 - \varepsilon_{\infty}}{1 + j\omega\tau 2}$$

The values of ε_1, ε_2, ε_{∞} and relaxation time τ_1 and τ_2 can be found from this table [5].

Table 2.1: Different parameters of permittivity and the relaxation time

Model	$\boldsymbol{\varepsilon_{\infty}}$	$\boldsymbol{\varepsilon_1}$	$\boldsymbol{\varepsilon_2}$	$\boldsymbol{\tau_1}$ **(ps)**	$\boldsymbol{\tau_2}$ **(ps)**
Water	3.3	78.8	4.5	8.4	0.1
Blood	2.1	130	3.8	14.4	0.1
Skin	3.0	60.0	3.6	10.6	0.2

In this thesis, we simulated relative permittivity against the Terahertz frequency (0.1-3THz) as to observe the behavior of permittivity in different human body skins, like dermis, epidermis and hypodermis layers and blood.

2.3 Path Loss

All together there are three parameters which are all frequency dependent in Terahertz channel namely Spreading Loss ($L_{spreading}$), Molecular absorption loss ($L_{Absorption}$) and Scattering loss ($L_{Scattering}$) [13].

$$\text{Path Loss} = PL_{spreading} * PL_{\text{Molecular Absorption}} * PL_{Scattering} \quad \text{.....(2.19)}$$

Expressing it in decibel yields to –

$$\text{Path Loss}_{dB} = PL_{spreading} + PL_{\text{Molecular Absorption}} + PL_{Scattering} \quad \text{.....(2.20)}$$

Spreading loss defines as loss which occurs when EM waves propagate through the medium. Molecular absorption loss defines as loss when EM waves propagate through different medium. In molecular absorption, EM energy is partially transformed into kinetic energy [1]. As different medium has different molecular structure, it varies from medium to medium. Lastly, scattering loss occurs when signal is scattered while propagating through the medium. But, the effect of scattering loss is negligible compared to spreading loss and molecular absorption loss. Path loss is expressed in decibel (dB). In this thesis, we only considered path loss because of spreading and molecular absorption. So total path loss yields to –

$$\text{Path Loss}_{dB} = PL_{spreading} + PL_{\text{Molecular Absorption}} \quad \text{.....(2.21)}$$

Expressing each of those component as decibel gives-

$$PL_{spreading} = -10 * \log_{10} (\text{Spreading coefficient}) \quad \text{.....(2.22)}$$

$$PL_{\text{Molecular Absorption}} = -10 * \log_{10} (\text{Molecular absorption coefficient}) \quad \text{.....(2.23)}$$

In our simulation we have used 1THz where frequency range of THz is (0.1-10THz).

Now,

$$\text{Attenuation (Loss)} = (4\pi k/\lambda_0) \quad \text{.....(2.24)}$$

where, λ_0 is the wavelength of the medium and k is attenuation coefficient.

Spreading coefficient = $(\lambda_1/4\pi d)^2$……...……(2.25)

where λ_1 is the wavelength of spreading coefficient.

Molecular absorption coefficient = $e^{-Attenuation*d}$ ……...……...…(2.26)

where d is the distance.

$\lambda_0 = c/f$ ……(2.27)

Here, f = 1THz and c is denoted as the speed of light and the value of $c = 3*10^8$ m/s.

$\lambda_1 = \lambda_0/n$ ……..(2.28)

Here, n is the refractive index.

2.4 Conductivity

Conductivity is defined as how easily and efficiently an electric charge or heat can pass through the medium. In wireless communication, skin conductivity plays a vital role as, if the skin conductivity is high then signal will be efficiently received by the medium and data can be easily and smoothly collected. In addition to that, increase in skin conductivity decreases the loss while the signal is propagating through the media. In other word, spreading loss, absorption loss and the scattering loss will be reduced. Conductivity is related to the penetration depth as we get the penetration depth by using conductivity. The more the conductivity, the more the penetration depth and the more efficient the system is. Conductivity is expressed by the unit σ (sigma) and its SI unit is Siemens per meter.

$\sigma = \varepsilon_{imaginary} * 2 * \pi * f * \varepsilon_0$ ……(2.29)

The value we used for the $\varepsilon_0 = 8.85 * 10^{-12}$F/m and f is the frequency and the value of f is in between 0.1 -3THz.

We simulate in terms of human skin composed of blood, water, epidermis, dermis and hypodermis. To protect the skin from all kind of contacts, epidermis form the utmost part of the skin. Dermis is found underneath the epidermis layer and it consists of various connective tissues, hair root, and nerve sensor. In addition to that, dermis is divided into two parts- one is called the papillary layer and the other is known as reticular layer. Underneath of dermis, there lies the core and thin part of the skin known as hypodermis and it stores various kinds of fats.

2.5 Nanotechnology Functionality in Terahertz Band

Wireless communication industry is embarking new edges in the field of nanosized devices. Nanotechnologies are now empowering nanosensors and nanoanodes. These, nanosensors are having extraordinary precision to identify different occurrence. Moreover, nanomachines, are capable of performing functions related to data storage for detection and actuation [14]. Currently, wireless nanonetworks have avalanche speed and outstanding accuracy in identification of diseases. Also, they are efficient for functioning in real time within the human body and will greatly benefit medical monitoring and communication with medical implants. Despite excellent advances in nanodevice technology, allowing communication between nanomachines remains a significant challenge [15].

Different communication methods are used in the operation of nanodevices, the finest method for information exchange is the use of wireless communication network (WCN) to function in the Terahertz spectral band using electromagnetic waves. Previously bands greatly lack one of the important features like size reduction. But nanosystems by Terahertz communication bandwidth thus make such systems an ideal desirable option for future body-centered communication applications. Minor differences in the water content of the body as well as biomaterial body tissues are efficiently detected by these nanodevices. That is because

of their brief wavelength (λ), terahertz radiation, and the presence of molecular resonances at these frequencies. Therefore, the assessment of electromagnetic propagation of terahertz band in human tissues is one promising increasing area in latest studies. This is to develop sophisticated diagnostic instruments to detect some anomalies early that indicate a severe disease such as skin cancer. Another benefit of working in a terahertz band is that it promotes a very elevated data transmission rate, almost equal to terabits per second (Tbps). Therefore, these underused spectral bands have reduced scattering and spreading impact.

Significant input of this underused spectral band to prospective future medical technologies is its benefits of offering radiation that is less prone to propagation impacts such as spreading loss, scattering impact, more genuine for data quality. It is also harmless on biological tissues and do not destroy human tissues.

Absorption is one of the prime reasons for heat reaction for human tissues induced by terahertz radiation. However, many suggestions have been suggested that by considering the parameters of terahertz exposure this effect can be decreased. In specific, the length of exposure using an ON-OFF method implies intermittent subjection to radiation. For molecular absorption in short distances, ON-OFF keying modulation system was subsequently suggested but this does not have a drastic effect on the transmission connection.

2.5.1 Terahertz Transmitter

Nanodevices need to be compact for interaction. That is, a maximum size area should be approximately hundred square nanometers or hundred square micrometers. The goal is to fortify that they are quick to bear gigahertz (GHz) bandwidth modulation for them. As well as they should be both coherent tunable [16].

As a consequence of contemporary sophisticated techniques, the various models and analysis displayed by electronic devices indicate that the devices could be feasible for biological sector. For instance, electronic devices can provide elevated average output energy at reduced THz frequencies [17]. Their features include the capacity to produce small line widths of ongoing THz radiation. Also functionality at ambient temperature, and compact, ragged both reinforce the findings [18].

For both Giga bit per second (Gbps) and Terabit per second (Tbps) connections ultra-broadband antennas are also required in the THz band. Therefore, the prospective of these antennas must be explored with regard to metamaterials and nanomaterials. Some previous studies show that, plasmonic nano-antennas are made of mainly grapheme. Because of their surface charging oscillation nature these graphene made antennas can therefore adjusted to be integrated with almost everything by means of material doping. The issue of attaining the above relies on how to characterize and the coupling and interaction effects of neighboring antennas [19].

2.5.2 Terahertz Receiver

Significant progress has been made in the sensitivity of the THz detector for over 70 years with a factor of 10 reducing the noise equivalent power (NEP) value. The reduction corresponds after every two years to the enhancement of a factor of two [14]. To surpass the extreme loss, detectors with high responsiveness for detection are needed and also for

utilizing THz band of high frequencies. Peak energy is measured in mW and μW range based on sensor type [20].

2.6 Intrabody Pathlosses

When an electromagnetic wave passes through the medium, a path-loss that depends on the frequency and the distance between the transmitter and the receiver is involved. Path loss or attenuation of the path is the decrease of an EM wave's power density (attenuation) as it propagates through space. On the other hand, if the THz band is exploited, the molecular absorption impact plays a significant part in the transmission. There are three primary frequency dependent parameters that are put up to the complete path loss for Terahertz band. These parameters are: L_{spr} (f) spreading loss, L_{abs}(f) molecular absorption loss, and L_{sca} (f) scattering loss. Whereas the factor of complete attenuation is expressed by:

$$L_{tot=}L_{spr}(f) \times L_{abs}(f) \times L_{sca}(f) \quad \text{(2.29)}$$

THz band is located between microwaves and millimeter waves.

2.6.1 Human Tissue's Wave Spreading Loss

EM wave propagation induce spreading loss and medium's absorption loss due to absorption. Now spreading loss can be expressed by:

$$L_{spr} = D\left(\frac{\lambda_r}{4\pi d}\right)^2 \quad \text{(2.30)}$$

Here λ_r, effective wavelength, is λ/n', n' and $n''$are real and imaginary parts of tissue refractive index n [8]. Now tissues' refractive index can be expressed by:

$$n = n' - jn'' \quad \text{(2.31)}$$

$n = \sqrt{\epsilon_r}$, here r stands for relative permittivity, is worth noting. Now relative permittivity is enumerated μ_r=1, since there is almost no magnetic conduct in biological tissues [21-22].

D, which symbolizes directivity adverts maximum gain of nanoantenna. It is provided by maximum power density's ratio $P(\theta, \Phi)max$ in W/m^2 to its average value which is calculated over a sphere as seen in an antenna's far field. Therefore,

$$D = \frac{P(\theta,\Phi)_{max}}{P(\theta,\Phi)_{avg}} \quad \text{(2.32)}$$

Directivity's final look is provided from [23] as:

$$D = \frac{4\pi}{\iint_{4\pi} P_n(\theta,\Phi)d\Omega} = \frac{4\pi}{\Omega_A} \quad \text{(2.33)}$$

Where,$P_n(\theta, \Phi)d\Omega = P(\theta, \Phi)/P(\theta, \Phi)_{max}$ is known as the normal energy pattern and Ω_A relates as solid angle of radiation which depends completely on the source and antenna's specific radiation pattern being used. Now as an instance, Ω_A is provided here as a directional source which is mainly beams narrow width. Now:

$$\Omega_A = \int_{\Phi=0}^{2\pi} \int_{\theta=0}^{\Delta\theta} \sin\theta \, d\theta \, d\Phi = 2\pi(1 - \cos\Delta\theta) \quad \text{(2.34)}$$

Considering a light source which is with a Gaussian beam and with radiation [24]:

$$E_\theta = \frac{1}{2}(1 + \cos\theta) \quad \text{(2.35)}$$

Now, P, which is radiated power is proportional to $|E_\theta|^2$. Now consequently $P = |E_\theta|^2/2\eta$ [11],[8]. Wave impedance η for human tissue medium, and Ω_A, the solid angle. Therefore Gaussian beam of width $\Delta\theta$ is expressed as:

$$\Omega_A = \int_{\Phi=0}^{2\pi} \int_{\theta=0}^{\Delta\theta} \frac{1}{4}(1 + 2\cos\theta + cos^2\theta) \sin\theta \, d\theta \, d\Phi$$

$$= \frac{\pi}{2}\left[\frac{8}{3} - \left(\cos\Delta\theta + cos^2\Delta\theta \cos\theta + \frac{1}{3}cos^3\Delta\theta\right)\right] \quad \text{(2.36)}$$

It is essential to remember that the big quantity of spreading loss is one of the Terahertz band's primary constraints. As a consequence, future nanodevices transmission range would be significantly reduced.

2.6.2 Pathloss in Human Tissue for Molecular Absorption

The phenomenon of molecular absorption triggers when the frequency chosen for the transmission of electromagnetic waves is about the same as the resonant frequency in molecules for internal vibration [17]. Then the energy absorbed is transformed into kinetic energy. The absorption of molecules relies on several variables such as temperature, atmospheric circumstances, molecular physical characteristics, etc. For a specified frequency, this phenomenon has no particular value.

The electromagnetic waves within the Terahertz at specific frequencies can excite any medium's molecules. Mainly translational and rotational movements appear in molecule. Also atoms inner movement is vibration that represents a regular movement. THz induces different vibration-oriented movements but they do not break the molecules. Kinetic energy will develop from propagating wave energy, which is due to this mentioned vibration. In communication, this quantity of transformed energy is considered as a loss. These absorption is deduced from incident fraction of the EM radiation which is having the capacity to surpass at particular frequency throughout the medium. With Beer-Lambert law [17], attenuation induced for molecular absorption due to EM wave traveling in distance d, is provided by:

$$L_{abs} = e^{-\mu_{abs} d} \quad \text{.....(2.37)}$$

Molecular absorption's coefficient is μ_{abs}. It relies on the medium structure and was initially introduced and calculated in [17] for gas molecules. The same strategy is pursued in the for intrabody communications. These also include chromophores that absorb light radiation in our tissues. Each molecule has an absorption spectrum that can alter rapidly even for tiny differences in wavelengths. The medium conveys non-uniformity of the refractive index [25]. For calculation coefficient using

$$\mu_{abs} = \frac{4\pi(n'')}{\lambda_g} \quad \text{.....(2.38)}$$

We can use two distinct approaches to assess the absorption coefficient. On one side, we can model individual particle absorption. The particles' absorption efficiency can be demonstrated

$$Q_{abs} = \sigma_{abs}/\sigma_g \quad (2.39)$$

where, $\sigma_{abs}$is the molecular absorption cross section, and σ_g is the geometric cross section. Now

$$\mu_{abs} = \rho_v Q_{abs} \sigma_g \quad (2.40)$$

Where ρ_v is the concentration of particles and is provided by $\rho_v = (\kappa/\frac{4}{3}\pi r^3)$, whereas κ is that particle's fraction volume. The primary challenge at this point is estimating Q_{abs}.

As long as we are dealing with a big amount of molecules, the effective medium hypothesis is commonly taken into account. In particular, following the Debye relaxation model and using equation (2.1), (2.2), (2.3), (2.4) for human tissues the dielectric response for frequency domain can be characterized. And that too with tissues with higher water content [26]. Multiple Debye procedures are feasible for a pure material when describing the complex permittivity [27].

Microstructure of biological matter as well as disordered nature and in such products as well as the supracellular organization, cause distinct polarization processes. Non-symmetric time-domain reaction and various relaxation times are also included. Complex permittivity for polar liquids at frequencies is up to 1 THz are provided by double Debye equations [28].

With table 2.1 we have calculated ϵ' and ϵ''. Again these are used for calculating [29] L_{abs} in [30] at the THz band owing to molecular absorption. It is observed that human fat has reduced Debye parameters for THz frequencies [26], [31]. Catalogs of optical properties of human tissue accessible are procured [32-33].

2.6.3 Pathloss due to Scattering in Human Tissue

By the perception of nanosensors in a comprehensive manner, the human body is aggregation of different particles, such as cells, antibodies and molecules with distinctive geometrical analytical structures having various electromagnetic properties. Hence, the important effect of Scattering on signal transmission owing to these constituent particles and their non-uniformity features is indeed mandatory to emphasize. In addition, it is needed to investigate the various variables such as the size, shape, refractive index of each type particle even the wavelength and the propagation of the wave [37]. Theoretical models suggested by Rayleigh and Mie explained the scattering phenomenon that affects minor spherical barriers extensively. This model is used when the propagated EM wave's wavelength exceeds the diameter of the substance [38]. However, if the diameter of the constituent material exceeds the wavelength, then the laws of reflection or geometric dispersion are implemented [37]. Scattering is shown in an event of a plane wave on a scattered particle situated at the origin of a spherical coordinate scheme [39].

Its intensity I_{sca}, is presented here as [40]:

$$I_{sca} = \frac{1}{(kr)^2} I_{inc} S(\theta, \varphi) \quad \text{.....(2.41)}$$

Where k is incident radiation factor.

$Iinc$ is the intensity of the incident. In general, in relation to the optical features of the particle (θ,), is considerably dependent on different main parameters such as the wavelength of the incident beam, the dimension and its defined shape [40]. With the intensity equation, it is mandatory to express the scattering loss both the scattering cross-section and the scattering efficient performance.

$$\sigma_{sca} = \frac{1}{(k)^2} \int_0^{2\pi} \int_0^{\pi} [S(\theta, \varphi)] \sin\theta \, d\theta \, d\varphi \quad \text{.....(2.42)}$$

Where amplitude of the scattered particle defined as

$$S(\theta,\varphi) = \frac{k^2}{4\pi}\int \quad e^{-ik\xi \sin\theta(\xi\cos\phi+\eta\sin\phi)}(1+\cos\theta)\, d\xi\, d\eta \ldots\ldots\ldots\ldots\ldots\ldots\ldots\ldots\ldots\ldots(2.43)$$

Because both have an analogous deflection configuration and the spherical object's amplitude is treated as if it is independent of the azimuthal angle to alleviate the complexity

$$S(\theta) = \frac{k^2}{4\pi}\int \quad e^{-ik\xi \sin\theta}(1+\cos\theta)\, d\xi\, d\eta \ldots\ldots\ldots\ldots\ldots\ldots\ldots\ldots\ldots\ldots\ldots\ldots(2.44)$$

The integral evaluation is shown in [40].

Equivalent to absorption, Q_{sca}, an indicator representing efficient scattering evaluation, which is defined as the ratio of the energy dispersed by the basic substance to the total energy concentrated in the incident beam, and diverted by the substance's geometric cross-sectional structure and expressed as:

$$Q_{sca} = \sigma_{sca}/\sigma_g \ldots\ldots\ldots\ldots\ldots\ldots\ldots\ldots\ldots\ldots\ldots\ldots\ldots\ldots\ldots\ldots\ldots\ldots\ldots\ldots\ldots\ldots(2.45)$$

Because these variables depend significantly on the size of the substance, it is necessary to address the significance of considering the scattering for both small and big substances.

2.7 Pathloss in Terahertz Biological Channel Model

The characterization of a biological channel in the THz band is suggested in this section. For establishing BANN as a reference scenario, the dorsum of hand is considered to be a framework of four layers among which each layer is compatible with a specific kind of organic tissue. From the evaluation of primary electrical characteristics of different forms of organic tissue at 1 THz, we calculate the complete path loss once and the channel structure is described.

In order to determine the accurate treatment for a complicated medical case, pathological data are collected with the help of Body Area Nano-Neworks (BANN) which are embedded nano-

machines instilled inside human body. These nanometric devices have the ability to communicate with each other as well as with the outlying micro/macro world. We are proposing a sequentially designed model that contains two kinds of nanodevices, designed conceptually as well. These are- (i) nanonodes that circulate in the bloodstream to collect data and (ii) a hand implanted nanorouter that the nanonodes exchange data with. The BANN gets connected to the outside world by a gateway via standard technologies like Bluetooth or WiFi.

2.7.1 Channel Structure

We will place an external portable device at the dorsum of hand to analyze the device which will work as a gateway. The nanorouter is fed by the gateway with ultrasounds and inserted into the skin to interact with the nanonodes placed in the bloodstream in constant motion. The organic formation of the dorsum of the side was thus considered to be a framework of multiple layers, similar to the structure suggested in [41], [42] functions to evaluate the path loss between the nanorouter and the nanonode. Composed of skin, the upper layer is divided into dermis and epidermis. In our research, we considered these two tissues one because they show very comparable electrical characteristics [43]. The back of the hand contains rather a thin layer of subcutaneous fat that forms the centre layer of the framework. Hence, this is one of the most appropriate portions of human body at which a BANN could be set up because the thinness of this layer makes the distance between the vein and the outside of human body shorter (Table 2.2). Blood forms the veins which are modeled by the reduced layer. This will recreate the scenario within the circulatory system in which the nanonode operates. It is mandatory for both the nanodevices to be embedded in a biocompatible capsule/ artificial cell before they get inserted into the human body as mentioned in [44]. The thickness of each tissue indicated in Table 2.2 was acquired from experimental measurements for the dorsum of the hand reported in science literature [45-48].

Table 2.2 Biological Tissue's thickness for hand

Biological Tissue	Thickness (cm)
Epidermis	0.019
Dermis	0.106
Subcutaneous Fat	0.006
Blood	0.120

In our model, the nanorouter is placed at the intersection point of dermis and epidermis because the thickness of skin makes the implantation easier. Additionally, in this model nanonode is placed in the middle of vein which not only helps it study more prevalent situation but also enables it to establish a communication with the nanorouter.

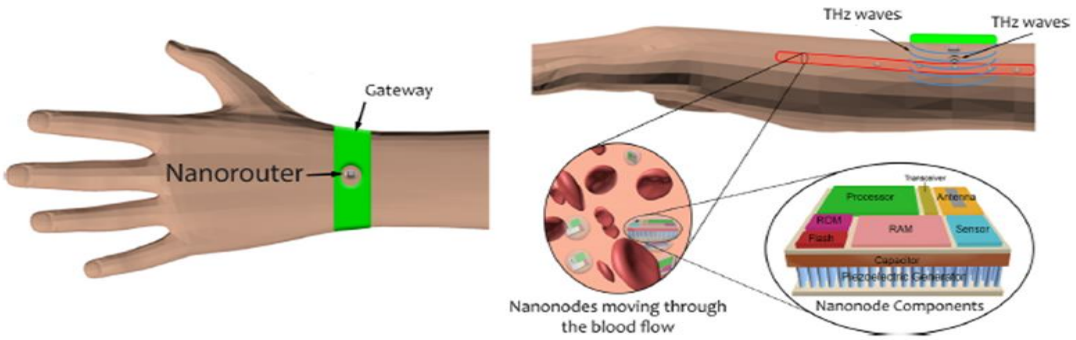

Figure 2.4: BANN Modeling for dorsum

2.7.2 Pathloss in Channel Model

Calculating the THz channel path loss in water vapor directed subsequent biological tissue pathloss research. Based on this strategy, a theoretical path loss model is suggested in [17] and the model formulates channel losses mainly considering spreading loss and molecular absorption loss. The first one reflects the transmission of the EM wave, which the Friis path loss formula can readily model and which we already showed in (2.29). Now we develop this equation for human hand:

$$L_{spr} = \left(\frac{4\pi d n_m}{\lambda_o}\right)^2 \text{.....(2.46)}$$

Where 'd' is the propagation distance, λ_o is the free-space wavelength (At frequency of 1 THz , λ_o= 300 μm), and n_m express the refractive index of the medium. After calculating we see that the spreading loss is comparatively high which limits the transmission range for nanoanodes severely. This concludes reduction of distance between the nanorouter and the nanonode significantly for human body.

The second term of the path loss accounts molecular absorption losses. This method relies on the frequency of work and the biological tissue being considered. Hence molecular absorption of each material can therefore be defined by the so-called absorption coefficient (α) from a mathematical point of view. It differs depending on the frequency. Now the expression can thus obtain the loss of the molecular absorption path provided (α).

$$L_{abs} = e^{-\mu_{abs} d} = e^{\alpha(\mathrm{f}) d} \text{.....(2.47)}$$

Where d is the propagation distance [48]. Once each term of the losses has been detailed, the total path loss of the channel can be expressed as follows (1):

$$L_{tot=} L_{spr}(f) \times L_{abs} = \left(\frac{4\pi d n_m}{\lambda_o}\right)^2 \times e^{\alpha(\mathrm{f}) d} \text{.....(2.48)}$$

Analyzing the previous equation, we can see as frequency, distance and absorption of the medium rises, corresponding pathloss also increases. Accurately in our thesis the total path loss for each tissue must be obtained as each will have a different effect on the path loss calculation owing to its particular refractive index and coefficient of absorption where it is possible to perceive enormous losses per unit of length. It is mentionable, that the work in [17], the losses due to by reflections in the interfaces between layers are not considered.

In our base scenario, when traveling through the dorsum of the hand, the nanonode could start the exchange of information with the nanorouter. Like the nanorouter, if nanoanodes are

near enough to the portal, they can generate energy from ultrasounds. Under these conditions, they send data to the shortest distance point with the router (SDP) during the time from the entry into the ultrasound region, where distance is minimum. The length of the ultrasound region, where ultrasound energy can be effectively extracted, was regarded a design parameter to be 5mmas. This duration is sufficient to guarantee that the ultrasound energy source is easily integrated into a tiny internal wearable device.

The distance between the transmitter and the receiver here relies on the distance between the nanonode and the SDP (Δd). The proportion of distance traveled through the skin (dskin), fat (dfat), and blood (dblood) by the EM wave also differs, directly affecting the complete pathloss. Applying basic trigonometry, d_{skin}, d_{fat} and d_{blood}as a function of Δd have been correspondingly determined:

$$d_{skin}(\Delta d) = \sqrt{t_{skin}^2 + (\Delta d \frac{t_{skin}}{d_{min}})^2} \quad \text{.....(2.49)}$$

$$d_{fat}(\Delta d) = \sqrt{(t_{skin} + t_{fat})^2 + (\Delta d \frac{t_{skin}+t_{fat}}{d_{min}})^2} - d_{skin} \quad \text{.....(2.50)}$$

$$d_{blood}(\Delta d) = \sqrt{d_{min}^2 + \Delta d^2} - (d_{fat} + d_{skin}) \quad \text{.....(2.51)}$$

Where $t_{skin}, t_{fat}, t_{blood}$ are the skin, fat, and blood thicknesses respectively, and d_{min} is the minimum distance between nanorouter and nanonode. Now the total path loss as the nanonode when it enters ultrasound region is less. It can be noted that the complete pathloss, reduces significantly as the nanonode enters the ultrasonic region (approaching the nanorouter) and reaches its minimum value. The nanonode is in the SDP if delta d is zero. But as the nanonode goes away from the SDP, the pathloss rises rapidly. Therefore, the nanonode should be triggered as near to the SDP as possible to enumerate the probability of finishing the communication without mistake.

Again the absorption phenomenon from the medium molecules not only impacts the attenuation characteristics of the channel, but also produces noise. This is the THz band's significant noise contribution. The intrinsic noise induced by graphene-based electronics devices (material suggested in most research to construct nanoantennas) can be regarded negligible.

2.8 Outage Probability

Outage probability is defined as the information rate being lower than the required information threshold rate. It is probability of an outage occurring within a specified time period.

WBANs are communication networks of sensor nodes (and/or actuators) that are positioned on, inside or around the human body, showing a fresh generation of WPAN (personal area network) and presenting several implementation difficulties. Compared to systems in the traditional WSN, sensor nodes in WBANs are tiny and integrated with finite source. Finite source limits the energy used by sensor nodes in information collection, processing, storage and delivery.

In WBAN many sensors are distributed evenly around the body to monitor the health status and each sensor collects and delivers information to the MN master node. Then MN sends its information to the monitor node, either analyzing the information obtained or transmitting the information to the physicians via the internet.

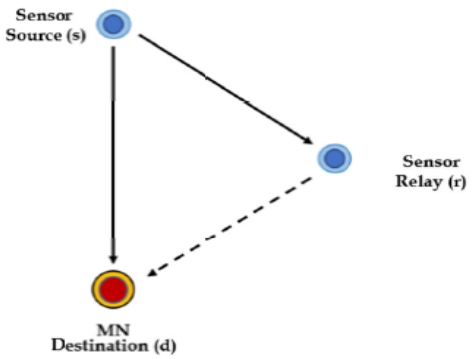

Figure 2.5: Master-node(MN) architecture

Distance between S and MN, S to R and R to MN are denoted as d_{sd}, d_{sr} and d_{rd}. Now taking the distance between sensor and MN as S-M link-

The signal-to noise ratio for S-M link is expressed as:

$$\gamma_{sd} = \frac{P_t \delta_c}{P_N} K_{sd} \quad \text{.....(2.52)}$$

Where P_t is the transmission power, δ_c is a multiplication of all antennas gain, P_N is the noise power and K_{sd} is the complex Gaussian random variable with unit variance. Therefore, the channel gain $|K_{sd}|^2$ is an exponential distributed random variable with the mean value, E $[|K_{sd}|^2]=d_{sd}^{-\alpha}$, where E denotes expectation, the d_{sd} is distance of the S – D link. The transmission rate over S - M link can be expressed as

$$\beta_{sd} = B \log_2(1 + \frac{P_t \delta_c}{P_N} K_{sd}) \quad \text{.....(2.53)}$$

Where B is the bandwidth of the transmission channel and is set to unity. The probability of outage is described as the probability that the speed of transmission is less than or equal to the necessary speed of transmission β_0.The outage probability can be expressed as

$$P_{sd}^{out} = P(\beta_{sd} \leq \beta_0) = 1 - \exp(-\frac{U_t}{P_t d_{sd}^{-\alpha}}) \quad \text{.....(2.54)}$$

Where, $U_t = P_N(2^{\beta_0} - 1)/\delta_c$. Consequently, the successful transmission probability of the S-M can be expressed as:

$$P_{sd}^{s} = 1 - P_{sd}^{out} = exp(-\frac{U_t}{P_t d_{sd}^{-\alpha}}) \quad \text{.....(2.56)}$$

For WBAN the outage probability for different mediums and different distances:

Source (skin, blood, fat) to destination:

P_0 = transmission power, δ_{c0}= channel gain, T_0 = required transmission rate,

Outage Probability, $P_{sd_{out}} = \Pr(T_{sd} \leq T_0) = 1 - \exp(-\left(\frac{\left(2^{\frac{T_0}{B}} - 1\right)}{P_{t0}}\right) * P_N * L_{path}))$..(2.57)

Source (skin, blood, fat) to Relay

P_{t1}= transmission power, δ_{c1}= channel gain, T_1= required transmission rate,

$$T_{sr} = B \log_2(1 + \frac{P_{t1}\delta_{c1}}{(\frac{4\pi d n_m}{\lambda_1})^2 e^{\alpha(f)d} * P_N})$$

Outage probability, $P_{sr_{out}} = \Pr(T_{sr} \leq T_1) = 1 - \exp(-\left(\frac{\left(2^{\frac{T_1}{B}} - 1\right)}{P_{t1}}\right) * P_N * L_{path}))$…(2.58)

Relay to destination

P_{t2}= transmission power, δ_{c2}= channel gain, T_2= required transmission rate,

$$T_{rd} = B \log_2(1 + \frac{P_{t2}\delta_{c2}}{L_{path}P_N})$$

Outage probability, $P_{rd_{out}} = \Pr(T_{rd} \leq T_2) = 1 - \exp(-\left(\frac{\left(2^{\frac{T_2}{B}} - 1\right)}{P_{t2}}\right) * P_N * L_{path}))$…(2.59)

The derivation in details for outage probability is given in Appendix A.

Chapter 3

Result and Discussion

3.1 Introduction

In this chapter, we have identified relative permittivity, sigma conductivity, power reflection coefficient (parallel and perpendicular), absorption coefficient, spreading coefficient, outage probability and pathloss of blood and plasma, water and skin (dermis and epidermis) and analyzed the results below each figure using MATLAB**.**

3.2 Plots and Discussion

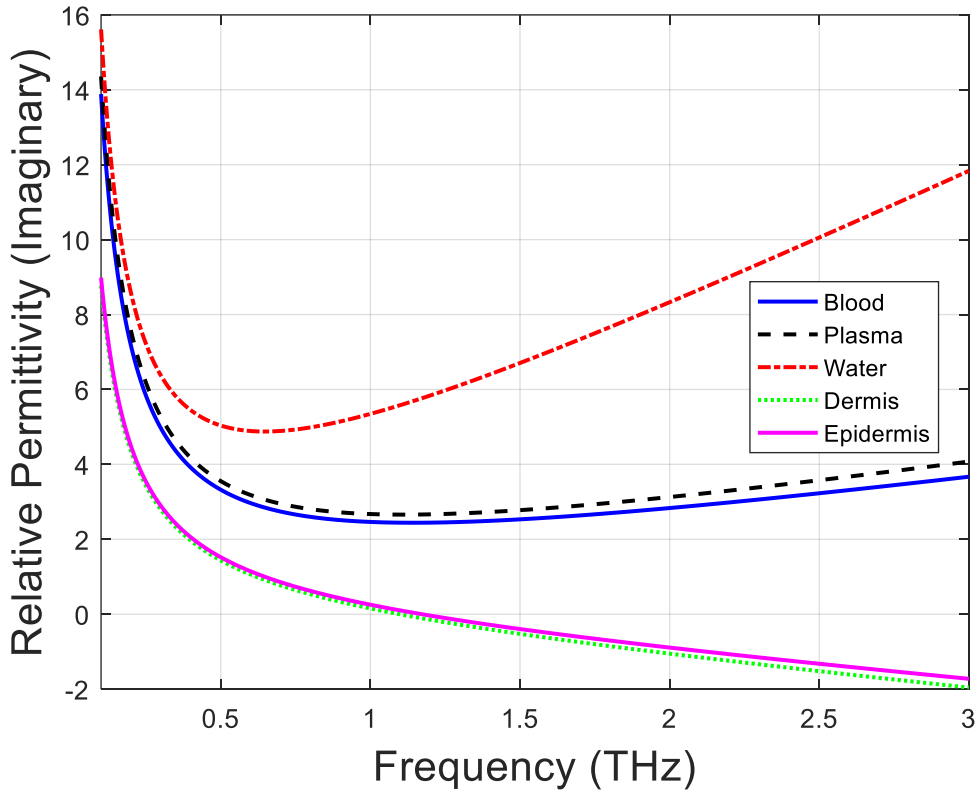

Figure 3.1: Relative Permittivity (Imaginary) vs. Frequency (THz)

From figure 3.1 we can see that at 1THz frequency the imaginary relative permittivity of blood is 2.463 while plasma, water, skin dermis and skin epidermis have an imaginary

relative permittivity of 2.673, 5.349, 0.153 and 0.2508 respectively at 1THz frequency. At 2THz frequency, the imaginary relative permittivity of blood, plasma, water, skin dermis and skin epidermis become 2.835, 3.129, 8.33, -1.055 and -0.892 respectively. So, at 1THz frequency water has the highest imaginary relative permittivity and skin dermis has the lowest imaginary relative permittivity. If the frequency increases the imaginary relative permittivity of water increases but the imaginary relative permittivity of skin dermis and skin epidermis decreases while it remains approximately same for blood and plasma.

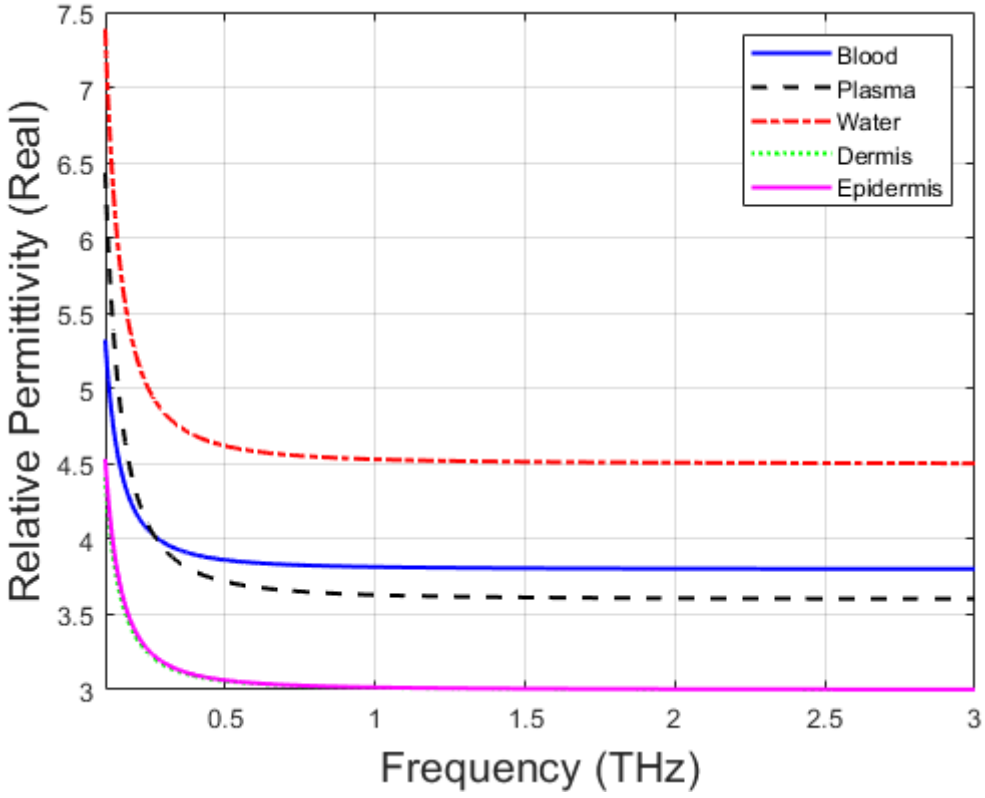

Figure 3.2: Relative Permittivity (Real) vs. Frequency (THz)

From figure 3.2 we can see that at 1THz frequency blood, plasma, water have the real relative permittivity of 3.815, 3.629, 4.53 respectively and skin dermis and skin epidermis have an equal real relative permittivity of 3.016 at 1THz frequency. This real relative permittivity becomes 3.804, 3.607, 4,507 and 3.004 for blood, plasma, water and skin (both dermis and epidermis) respectively at 2THz frequency. We can see that both at 1THz and 2THz

frequencies, water has the highest real relative permittivity and skin has the lowest real relative permittivity. As the frequency increases the real permittivity of all elements starts decreasing exponentially up to 0.5THz frequency. After 0.5THz the real permittivity of all elements tend to be constant as the frequency increases.

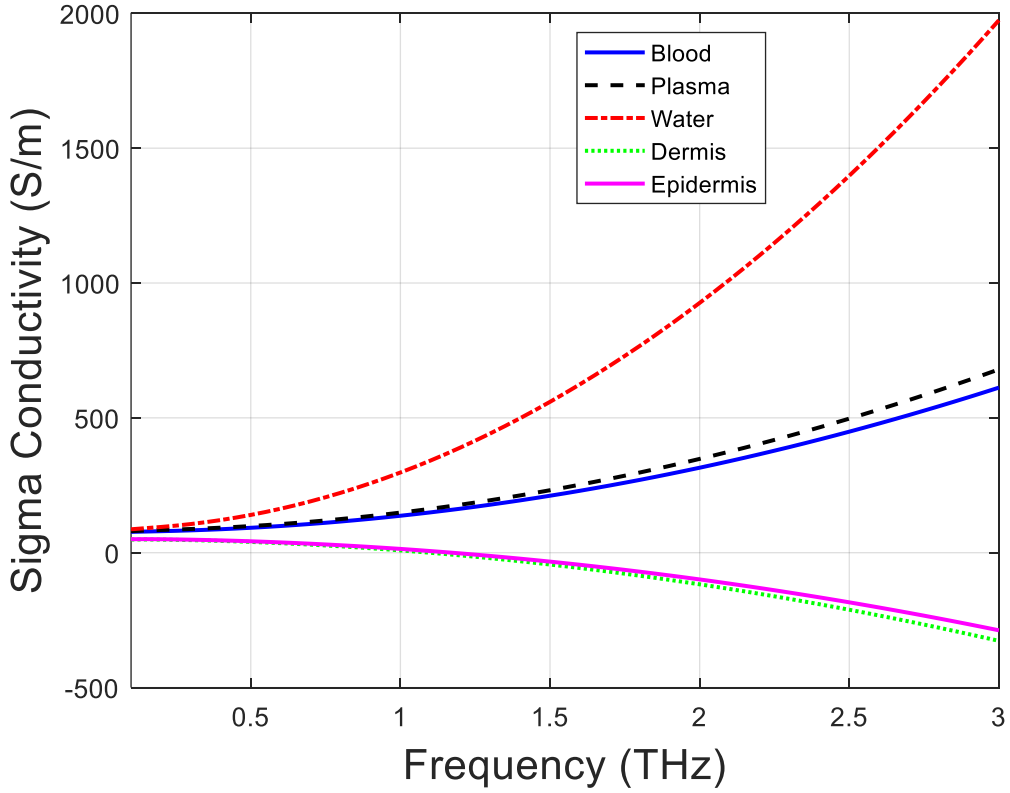

Figure 3.3: Sigma Conductivity (S/m) vs. Frequency (THz)

From figure 3.3 we can see that at 1THz frequency blood, plasma, water, skin dermis and skin epidermis have sigma conductivity of 136.9 S/m, 148.7S/m, 294.7S/m. 8.506 S/m and 14.03 S/m respectively. The sigma conductivity becomes 315.1 S/m, 347.8 S/m, 926.3 S/m, -117.3 S/m, -99.16 S/m for blood, plasma, water, skin dermis and skin epidermis respectively at 2THz frequency. At both frequencies water has the highest sigma conductivity and skin dermis has the lowest sigma conductivity. As the frequency increases the sigma conductivity of blood, plasma, water increases while the sigma conductivity of skin (both dermis and epidermis) decreases.

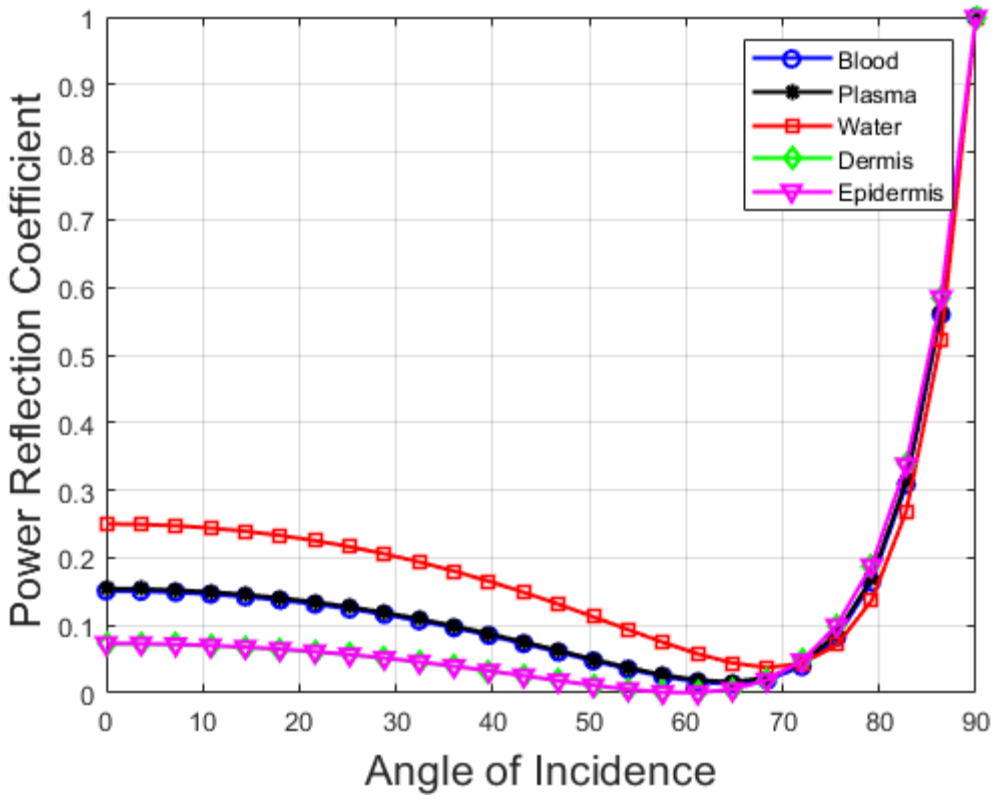

Figure 3.4: Parallel Power Reflection Coefficient vs. Angle of Incidence (degree)

From figure 3.4 we can see that for an angle of incidence of 28.8° the parallel power reflection coefficients of blood and plasma, water, skin (dermis and epidermis) are 0.1191, 0.2058 and 0.05128 respectively. If the angle increases to 61.2° then the parallel power reflection coefficient of blood, water, skin becomes 0.01913, 0.05786 and 0.000432 respectively. However, all elements have the highest parallel power reflection coefficient of 1 for an angle of incidence of 90°.

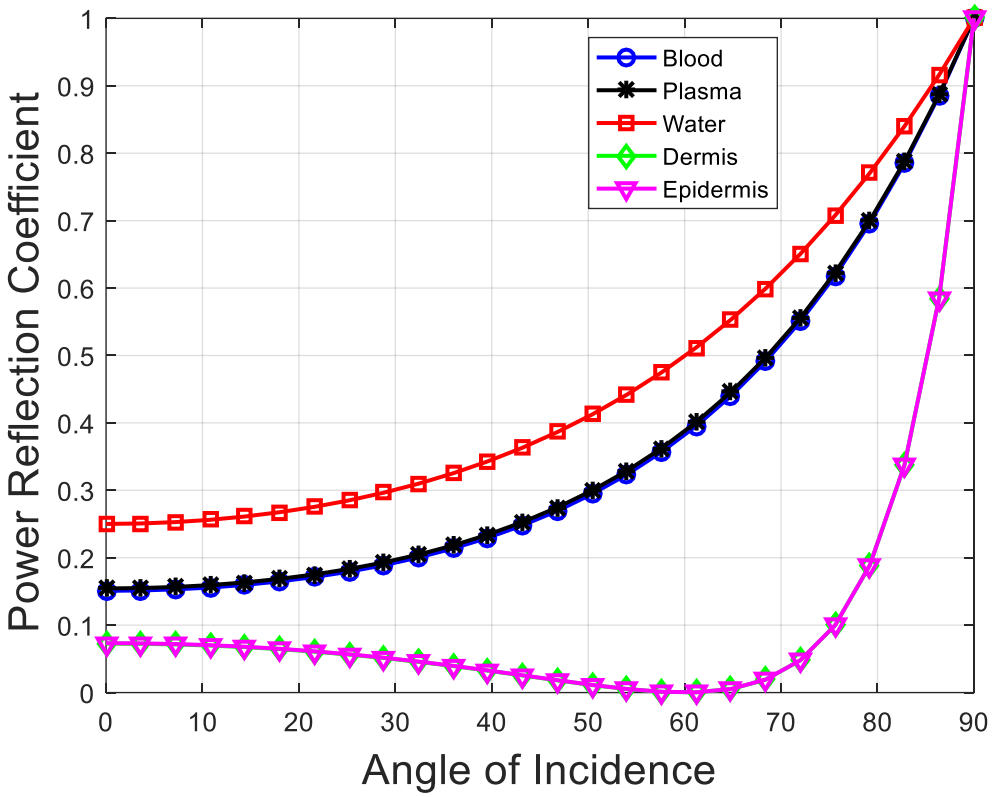

Figure 3.5: Perpendicular Power Reflection Coefficient vs. Angle of Incidence (degree)

From figure 3.5 we can see that for an angle of incidence of 28.8° the perpendicular power reflection coefficients of blood and plasma, water, skin (dermis and epidermis) are 0.193, 0.2965 and 0.05175 respectively. If the angle increases to 61.2° then the perpendicular power reflection coefficients of blood, water, skin becomes 0.401, 0.5118 and 0.000432 respectively. However, all elements have the highest perpendicular power reflection coefficient of 1 for an angle of incidence of 90°.

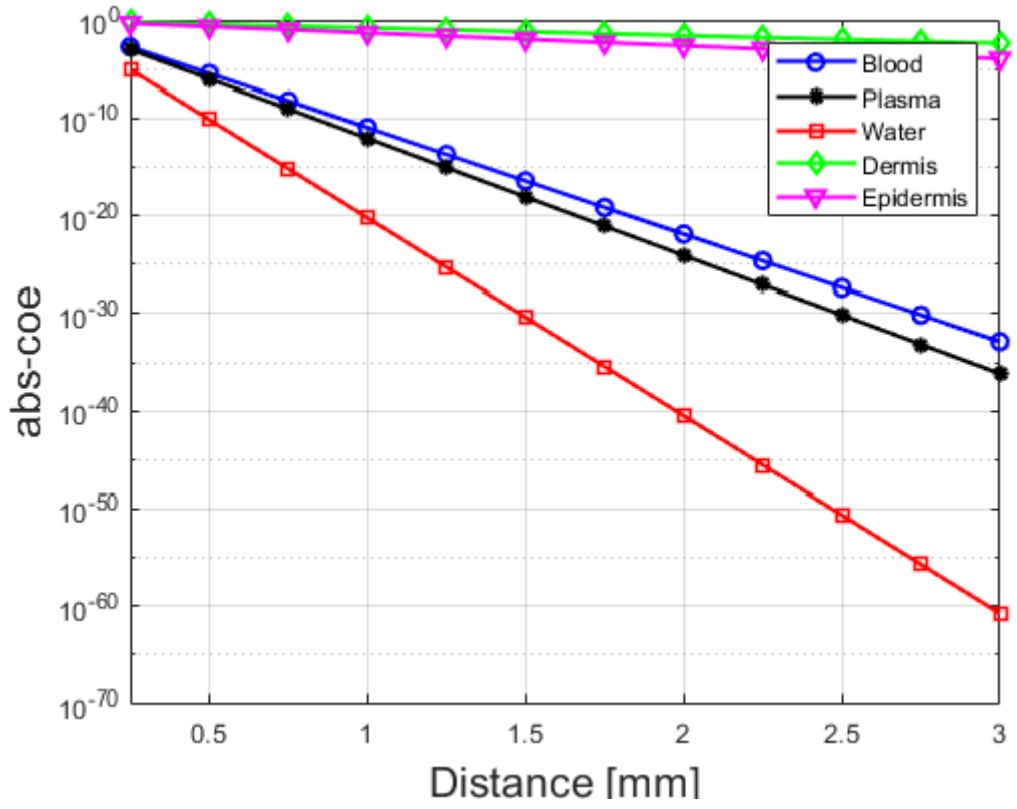

Figure 3.6: Absorption Coefficient vs. Distance (mm)

From figure 3.6 we can see that for 1 mm of distance blood, plasma, water, skin dermis and skin epidermis have absorption coefficient of 1.099×10^{-11}, 8.804×10^{-13}, 5.5609×10^{-21}, 0.1581, 0.04778 respectively. If the distance increases to 2 mm the absorption coefficients of blood, plasma, water, skin dermis, skin epidermis become 1.208×10^{-22}, 7.751×10^{-25}, 3.146×10^{-41}, 0.02499 and 0.002283. We can see that as the distance increases absorption coefficients of blood, plasma, water and skin decrease linearly. However, skin (dermis and epidermis) has the highest absorption coefficient at both distances.

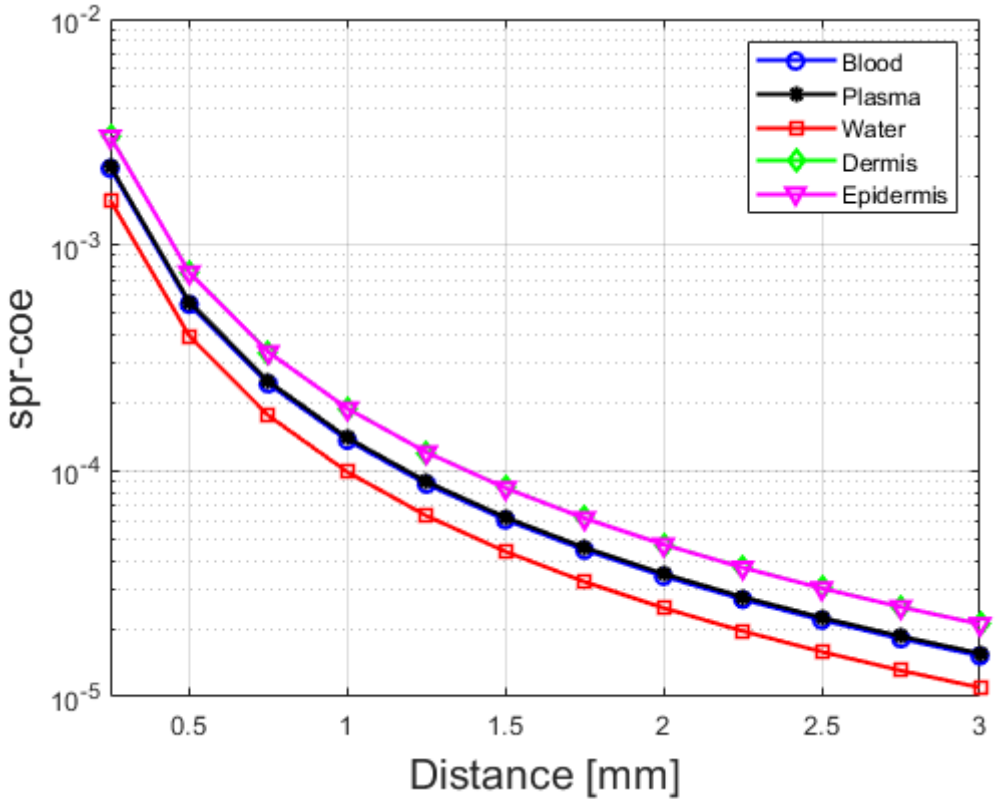

Figure 3.7: Spreading Coefficient vs. Distance (mm)

From figure 3.7 we can see that for 1 mm of distance whole blood and plasma, water, skin (dermis and epidermis) have spreading coefficient of 0.0001401, 9.879×10^{-4}, 0.0001887 respectively. If the distance increases to 2 mm the absorption coefficients of blood (blood and blood plasma), water, skin (dermis and epidermis) become 3.502×10^{-5},2.47×10^{-5}, 4.716×10^{-5} respectively. We can see that as the distance increases absorption coefficients of blood, plasma, water and skin decrease. However, skin (dermis and epidermis) has the highest absorption coefficient at both distances.

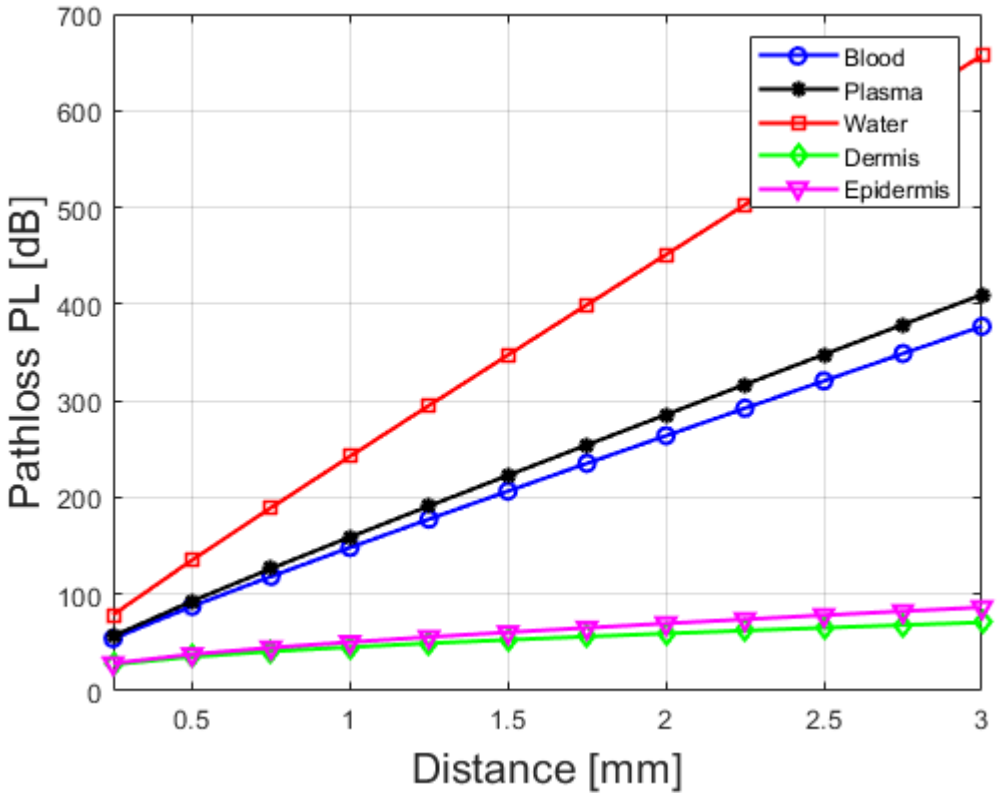

Figure 3.8: Pathloss (dB) vs. Distance (mm)

From figure 3.8 we can see that for 1 mm of distance blood, plasma, water, skin dermis and skin epidermis have a pathloss of 148.2 dB, 159.1 dB, 242.6 dB, 45.25 dB and 50.45 dB respectively. If the distance increases to 2 mm pathloss of blood, plasma, water, skin dermis and skin epidermis become 263.9 dB, 285.7 dB, 451.1 dB, 59.28 dB and 69.68 dB respectively. We can see that as the distance increases pathloss of all elements increase linearly. However, the fact that skin (dermis) has the lowest pathloss makes it appropriate for implantation of nanodevice.

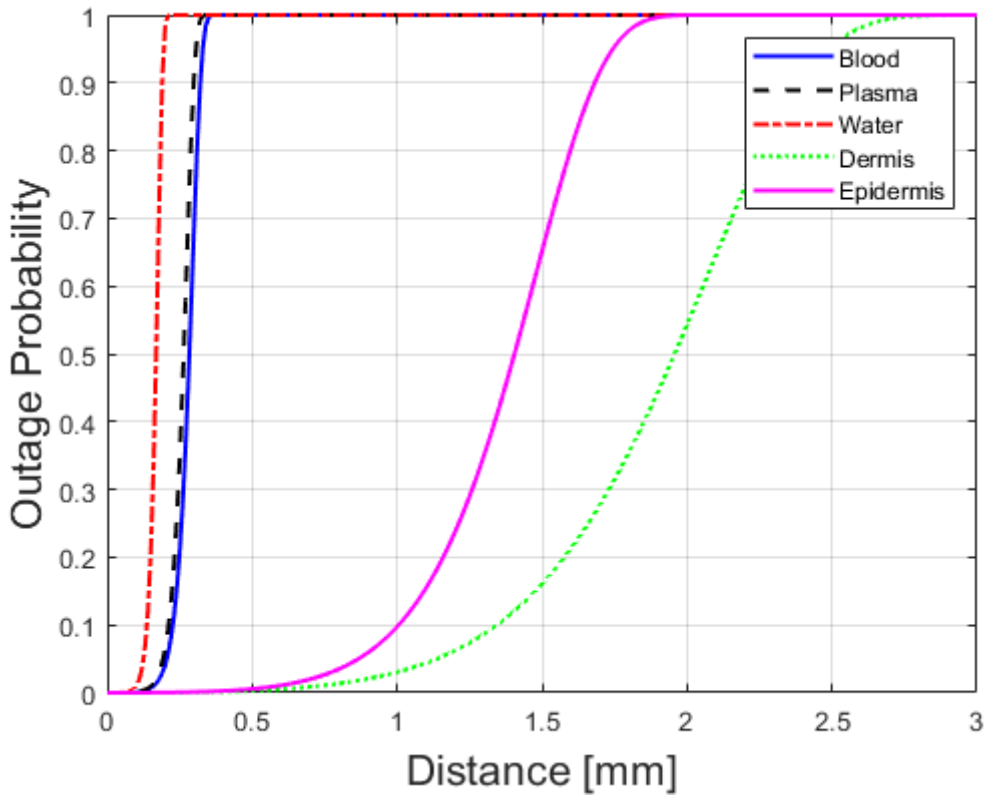

Figure 3.9: Outage Probability vs. Distance (mm)

From figure 3.9 we can see that for 1 mm of distance blood, plasma, water have an equal outage probability of 1 while skin dermis and skin epidermis have an outage probability of 0.03047 and 0.09744 respectively. We can see that the outage probability of blood, plasma and water increases exponentially as the distance increases up to 0.5 mm. As the distance goes beyond 0.5 mm the outage probability of blood, plasma and water becomes constant. For distance 2 mm the outage probability of skin dermis and skin epidermis becomes 0.543 and 1. Outage probability of skin also increases exponentially as the distance increases.

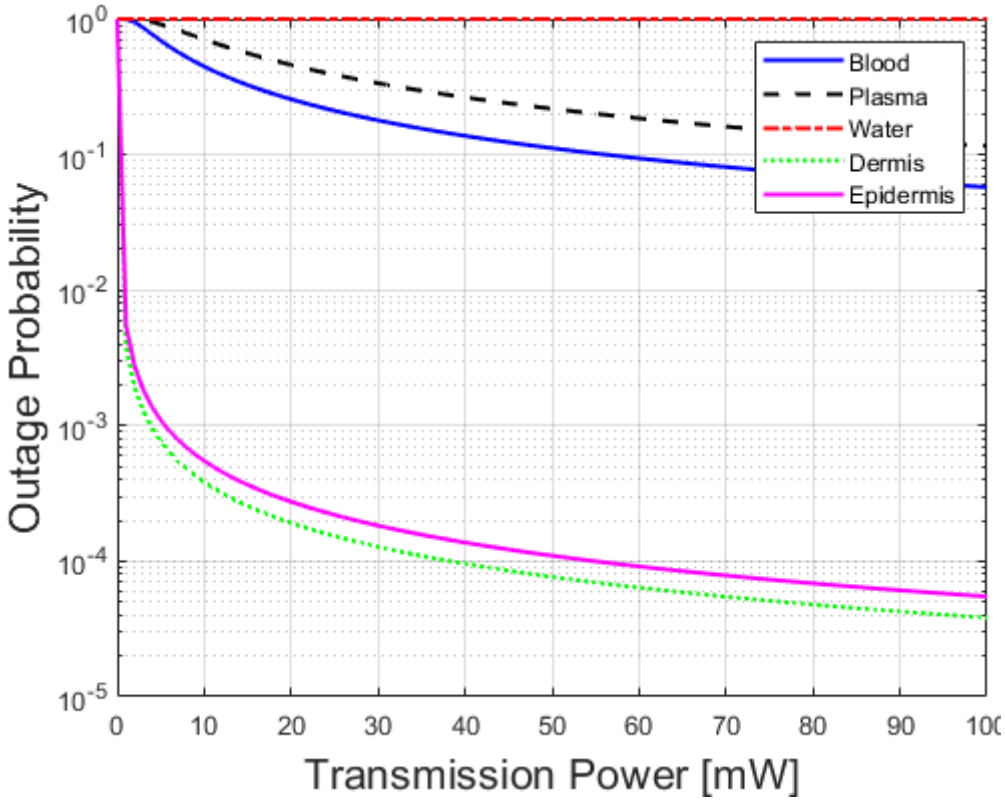

Figure 3.10: Outage Probability vs. Transmission Power (mW)

We can see that outage probability of water does not vary with the variations in transmission power. Water's outage probability is independent of transmission power. For 50 mW of transmission power the outage probability of blood, plasma, skin dermis and skin epidermis is 0.1115, 0.2178, 7.656×10^{-5} and 0.0001098 respectively. As the transmission power increases the outage probability of blood and skin decreases exponentially.

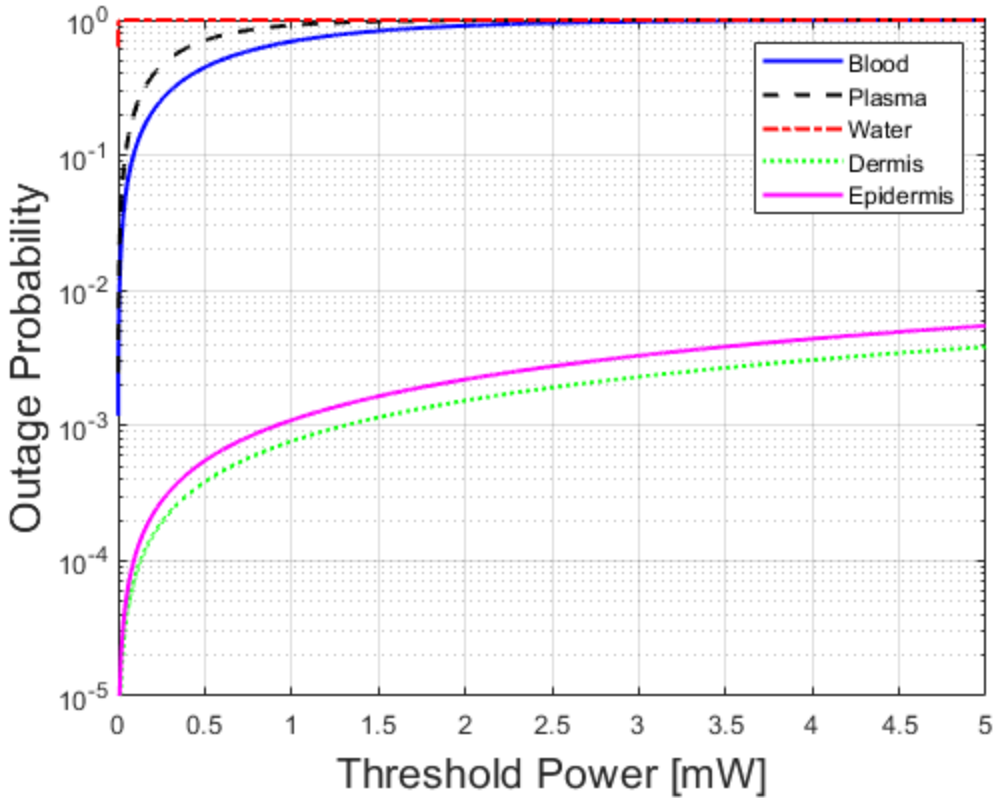

Figure 3.11: Outage Probability vs. Threshold Power (mW)

We can see that outage probability of water does not vary with the variations in threshold power. Water's outage probability is independent of threshold power. For 2.5 mW of threshold power the outage probability of blood, plasma, skin dermis and skin epidermis is 0.947, 1, 0.001913 and 0.002741 respectively. As the threshold power increases the outage probability of blood and skin increases. However, the outage probability of blood (blood and blood plasma) continues to increase up to the threshold power of 2.5 mW. When the threshold power exceeds 2.5mW the outage probability of blood tends to become a constant value of 1.

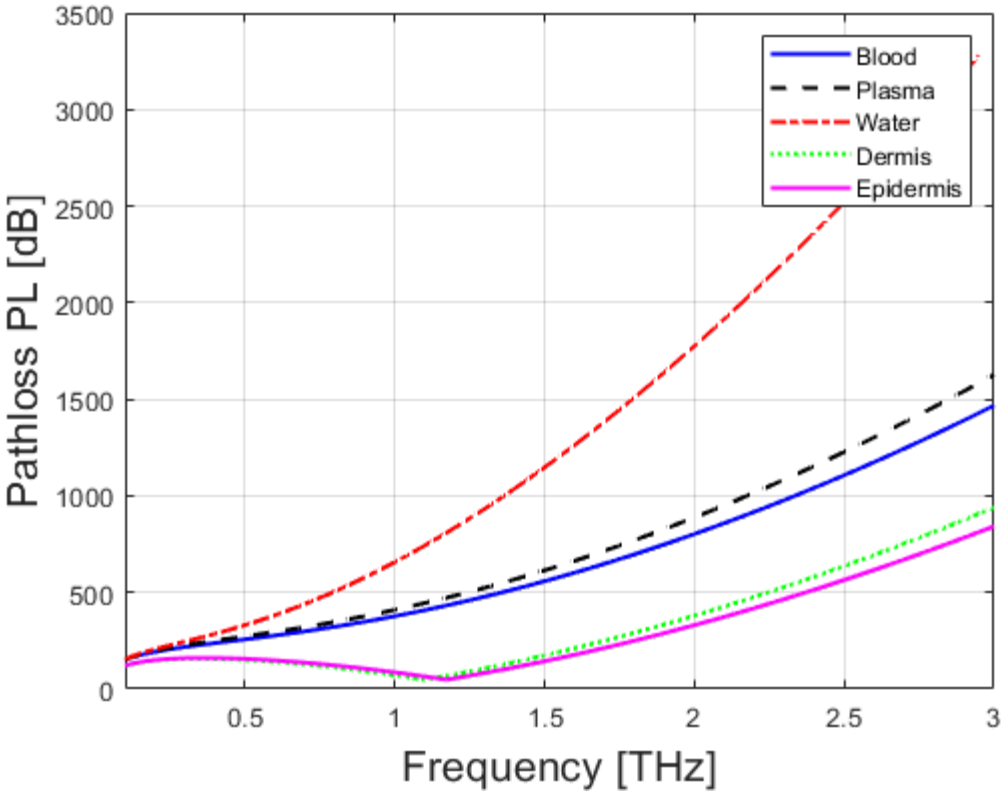

Figure 3.12: Pathloss (dB) vs. Frequency (THz)

From figure 3.12 we can see that for 1THz frequency blood, plasma and water have a pathloss of 377 dB, 409.7 dB, and 657.1 dB respectively while skin dermis and skin epidermis have an equal pathloss of 86.41 dB. If the frequency increases to 2THz, pathloss of blood, plasma, water, skin dermis and skin epidermis become 802.4 dB, 888 dB, 1776 dB, 380.1 dB and 330.6 dB respectively. We can see that as the frequency increases path loss of all elements increase exponentially. However, the fact that skin (epidermis) has the lowest pathloss makes it appropriate portion of human body at which a nanodevice could be set up.

Chapter 4

Conclusion

- In this thesis, we have performed analysis of nanoscale communication network for biomedical application.
- In biomedical application, wireless communication network using nanotechnology is being used for the transfer of information inside the human body, such as diagnostics, surgical operations, drug delivery etcetera. The information can be transmitted by electrons, electromagnetic waves or molecules, using the circulatory system as the medium.
- For effective transmission, we have studied the permittivity and relative permittivity of the medium, such as water, fat, hemoglobin, skin etcetera. For example, we have found that blood, plasma and water have the real relative permittivity of 3.815, 3.629 and 4.53 respectively while skin dermis and skin epidermis have an equal real relative permittivity of 3.016 at 1THz frequency.
- We have also studied the losses that might occur during the transmission through the medium, such as spreading loss, molecular absorption loss and scattering loss, together known as path loss. For example, for a distance of 1 mm skin has a pathloss of 45.25 dB. Now if we increase the distance to 2 mm the pathloss also increases to 59.28 dB.
- The main aim of our thesis was to investigate the behavior of different factors inside the human body for Terahertz (THz) band. For this, we have analyzed a gateway device which was laid at the dorsum of hand to review the intra-body path loss parameters.

4.1 Limitations

In nanoscale communication there lie a number of limitations and we found this while working in this thesis. Namely-

- Higher modulation is not much effective as signals get corrupted and the effect of noise adds to it while transmitting the signal inside the human body. Various kinds of modulation techniques are being considered but the expected data rate and energy conversation is not proved to be effective. So, there always lies a trade between those while considering higher modulation. Higher modulation should be increased as well as the efficiency.
- One of the main limitations is its range of communication. In nanoscale communication, communication occurs between a very less distances and so it is not feasible for a relatively higher distance. For this, we cannot just use the communication network anywhere so it must be placed very near to the human body. For a very small distance, communication is proved to be very much efficient but as the distance increases, the efficiency gets reduced. As a result, the production cost becomes a concerning issue.

4.2 Future Work

There are few areas in nanoscale communication where we can work in future to improve the performance to increase the efficiency and feasibility. Those are-

- Energy harvesting in nanoscale communication network needs improvement and there are a very limited number of energy harvesting process. Energy harvesting is a big issue in a way that the communication happens between a very short distance and part of the energy supplied to human body gets lost due to the reasons already discussed in this thesis earlier. To transfer the signal packet as well as harvesting energy at the same time is a challenging task. So, to work on the energy harvesting process is our main future goal.
- The selection of antenna is another important aspect to work on as in nanoscale communication, antenna must be very small but should be very much efficient in transmission and reception of signal. Use of different kind of microcontroller may be used to reduce the size of antenna which we call nanoantenna. In absence of a better nano antenna the efficiency and feasibility will be very much affected so this is also an important aspect to work in future.
- Battery free communication can also be a very efficient work for us in future as battery cost is very high and it needs to be replaced frequently. To power on different sensors, a high amount power gets lost. So, we want to replace the battery so that we can power on different sensor with almost zero power is one of our future goals.

REFERENCES

[1] R. Zhang, K. Yang, Q. H. Abbasi, K. A. Qaraqe, and A. Alomainy, “Analytical modelling of the effect of noise on the terahertz in-vivo communication channel for body-centric nano-networks”, Nano Communication Networks, vol. 15, pp . 59–68, 2018.

[2] S. Canovas-Carrasco, A.-J. Garcia-Sanchez, and J. Garcia-Haro, “A nano-scale communication network scheme and energy model for a human hand scenario”, Nano Communication Networks, vol. 15, pp. 17–27, 2018.

[3] A. Galal and X. Hesselbach, “Nano-networks communication architecture: Modeling and functions”, Nano Communication Networks, vol. 17, pp. 4562, 2018.

[4] R. Zhang, K. Yang, Q. H. Abbasi, K. A. Qaraqe, and A. Alomainy, “Analytical characterization of the terahertz in-vivo nano-network in the presence of interference based on ts-ook communication scheme”, IEEE Access, vol. 5, pp. 10 172–10 181, 2017.

[5] H. Elayan, R. M. Shubair, J. M. Jornet, and P. Johari, “Terahertz channel model and link budget analysis for intra body nanoscale communication”, IEEE Transactions on NanoBioscience, vol. 16, no. 6, pp. 491–503, Sep. 2017.

[6] D. B. Smith and L. W. Hanlen, “Channel modeling for wireless body area networks”, in Ultra-Low-Power Short-Range Radios, P. P. Mercier and A. P. Chandrakasan, Eds. Cham: Springer International Publishing, 2015, pp. 2555.

[7] Q. H. Abbasi, A. A. Nasir, K. Yang, K. A. Qaraqe, and A. Alomainy, “Cooperative in-vivo nano-network communication at terahertz frequencies”, IEEE Access, vol. 5, pp. 8642–8647, 2017.

[8] J. Lee and S. Kim, “Emergency-prioritized asymmetric protocol for improving qos of energy constraint wearable device in wireless body area networks”, Applied Sciences, vol. 8, no. 1, 2018.

[9] P. Kaythry, R. Kishore, and V. Praveena, “Energy efficient raptor codes for error control in wireless body area networks”, Wireless Personal Communications, vol. 103, no. 2, pp. 1133–1151, Nov. 2018.

[10] K. Tsujimura, K. Umebayashi, J. Kokkoniemi, J. Lehtom¨aki, and Y. Suzuki,“A causal channel model for the terahertz band”, IEEE Transactions on Terahertz Science and Technology, vol. 8, no. 1, pp. 52–62, Jan. 2018.

[11] A. K. Vavouris, F. Dervisi, V. Papanikolaou, P. Diamantoulakis, G. Karagiannidis, and S. Goudos, “An energy efficient modulation scheme for body-centricterahertz (THz) nanonetworks”, Jan. 2019.

[12] N. Tadashi, M. Moore, E. Akihiro, & S. Tatsuya (2008). Recent Research and Development in Molecular Communication Technology. *Journal of the National Institute of Information and Communications Technology*, *55*(4).

[13] M.S. Youssef, F.I. Ghanim, N. Imad, A.A. Alqasim, R. M. Shubair, “Design of Intra-body Nano-communication Network for Future Nano-medicine’’ *Technical Report*. Sep. 2018.

[14] I. F. Akyildiz, J. M. Jornet, and M. Pierobon, “Nanonetworks: A new frontier in communications,” Commun. ACM, vol. 54, no. 11, pp. 84–89, Nov. 2011.

[15] R. M. Shubair and H. Elayan, “*In vivo* wireless body communications: State-of-the-art and future directions,” in *Proc. LoughboroughAntennasPropag. Conf. (LAPC)*, Nov. 2015, pp. 1–5.

[16] L. P. Gin´e and I. F. Akyildiz, “Molecular communication options for long range nanonetworks,” *Computer Networks*, vol. 53, no. 16, pp. 2753–2766, 2009.

[17] J. M Jornet, I. F. Akyildiz, “*Channel Modeling and Capacity Analysis for Electromagnetic Wireless Nanonetworks in the Terahertz Band*.” IEEE Transactions on Wireless Communications, VOL.10, N0.10:3211-3221,2011.

[18] I. A. Ibraheem, N. Krumbholz, D. Mittleman, and M. Koch, “Low-dispersive dielectric mirrors for future wireless terahertz communication systems,” *IEEE microwave and wireless components letters*, vol. 18, no. 1, pp. 67–69, 2008.

[19] R. M. Goody and Y. L. Yung, *Atmospheric radiation: theoretical basis*. Oxford University Press, 1995.

[20] J. Wilkinson, “Nanotechnology applications in medicine.” Medical device technology, vol. 14, no. 5, pp. 29–31, 2003.

[21] A. Vander Vorst, A. Rosen, and Y. Kotsuka, *RF/Microwave Interaction with Biological Tissues*, vol. 181. Hoboken, NJ, USA: Wiley, 2006.

[22] P. Stavroulakis, *Biological Effects of Electromagnetic Fields*. Springer, 2003.

[23] C. A. Balanis, *Antenna Theory: Analysis and Design*. Hoboken, NJ, USA: Wiley, 2016.

[24] H. Lin, C. Fumeaux, B. M. Fischer, and D. Abbott, “Modelling of sub-wavelength THz sources as Gaussian apertures,” *Opt. Exp.*, vol. 18, no. 17, pp. 17672–17683, 2010.

[25] F. Martelli, S. Del Bianco, A. Ismaelli, and G. Zaccanti, “Light propagation through biological tissue and other diffusive media: Theory, solutions, and software,” *Proc. SPIE*, vol. 193, p. 298, Dec. 2009.

[26] K. M. Yaws, D. G. Mixon, and W. P. Roach, “Electromagnetic properties of tissue in the optical region,” *Proc. SPIE*, vol. 6435, p. 643507, Feb. 2007.

[27] J. Xu, K. W. Plaxco, and S. J. Allen, “Probing the collective vibrational dynamics of a protein in liquid water by terahertz absorption spectroscopy,” *Protein Sci.*, vol. 15, no. 5, pp. 1175–1181, 2006.

[28] J. Kindt and C. A. Schmuttenmaer, “Far-infrared dielectric properties of polar liquids probed by femtosecond terahertz pulse spectroscopy,” *J. Phys. Chem.*, vol. 100, no. 24, p. 10373, 1996.

[29] J. Xu, K. W. Plaxco, and S. J. Allen, “Absorption spectra of liquid water and aqueous buffers between 0.3 and 3.72 THz,” *J. Chem. Phys.*, vol. 124, no. 3, p. 36101, 2006.

[30] P. Biagioni, J.-S. Huang, and B. Hecht, “Nanoantennas for visible and infrared radiation,” *Rep. Progr. Phys.*, vol. 75, no. 2, p. 024402, 2012.

[31] C. B. Reid, G. Reese, A. P. Gibson, and V. P. Wallace, “Terahertz time-domain spectroscopy of human blood,” *IEEE J. Biomed. Health Informat.*, vol. 17, no. 4, pp. 774–778, Jul. 2013.

[32] R. M. Pope and E. S. Fry, “Absorption spectrum (380–700 nm) of pure water. II. Integrating cavity measurements,” *Appl. Opt.*, vol. 36, no. 33, pp. 8710–8723, 1997.

[33] R. L. van Veen, H. Sterenborg, A. Pifferi, A. Torricelli, and R. Cubeddu, “Determination of VIS- NIR absorption coefficients of mammalian fat, with time- and spatially resolved diffuse reflectance and transmission spectroscopy,” in *Proc. Biomed. Topical Meet.*, 2004, paper. SF4.

[34] J. A. McGrath, R. A. J. Eady, and F. M. Pope, *Anatomy and Organization of Human Skin*. Oxford, U.K.: Blackwell, 2008, pp. 45–128.

[35] F. A. Duck, *Physical Properties of Tissues: A Comprehensive Reference Book*. San Diego, CA, USA: Academic, 2013.

[36] Q. H. Abbasi, H. El Sallabi, N. Chopra, K. Yang, K. A. Qaraqe, and A. Alomainy, “Terahertz channel characterization inside the human skin for nano-scale body-centric networks,” *IEEE Trans. THz Sci. Technol.*, vol. 6, no. 3, pp. 427–434, May 2016.

[37] O. V. Salata, “Applications of nanoparticles in biology and medicine,” Journal of nanobiotechnology, vol. 2, no. 1, p. 1, 2004.

[38] E. S. Foundation and E. M. R. Councils, Nanomedicine: An ESF-European Medical Research Councils (EMRC) Forward Look Report, ser. Forward Look report. ESF, 2005.

[39] R. A. Freitas, “Current status of nanomedicine and medical nanorobotics,” Journal of Computational and Theoretical Nanoscience, vol. 2, no. 1, pp. 1–25, 2005.

[40] S. Sarkar and S. Misra, “From micro to nano: The evolution of wireless sensor-based health care,” IEEE Pulse, vol. 7, no. 1, pp. 21–25, Jan 2016.

[41] K. Yang, A. Pellegrini, M.O. Munoz, A. Brizzi, A. Alomainy, Y. Hao, Numerical analysis and characterization of THz propagation channel for body-centric nano-communications, IEEE Trans. Terahertz Sci. Technol. 5 (2015) 419–426.

[42] G. Piro, P. Bia, G. Boggia, D. Caratelli, L.A. Grieco, L. Mescia, Terahertz electromagnetic field propagation in human tissues: A study on communication capabilities, Nano Commun. Netw. 10 (2016) 51–59.

[43] E. Berry, A.J. Fitzgerald, N.N. Zinov’ev, G.C. Walker, S. Homer-Vanniasinkam, C.D. Sudworth, R.E. Miles, J.M. Chamberlain, M.A. Smith, Optical properties of tissue measured using terahertz-pulsed imaging, in: Proc. SPIE Phys. Med.Imaging, 2003, p. 459.

[44] M. Donohoe, S. Balasubramaniam, B. Jennings, J.M. Jornet, Powering in-body nanosensors with ultrasounds, IEEE Trans. Nanotechnol. 15 (2016) 151–154.

[45] G.C.R. Melia, M.P. Robinson, I.D. Flintoft, Development of a layered broadband model of biological materials for aerospace applications, in: EMC Eur. 2011 York, York, UK, n.d.: pp. 84–89.

[46] Y. Lee, K. Hwang, Skin thickness of Korean adults, Surg. Radiol. Anat. 24 (2002) 183–189.

[47] J.S. Petrofsky, M. Prowse, E. Lohman, The influence of ageing and diabetes on skin and subcutaneous fat thickness in different regions of the body, J. Appl. Res. 8 (2008) 55–61.

[48] A.O. Alradi, S.G. Carruthers, Evaluation and application of the linear variabledifferential transformer technique for the assessment of human dorsal hand vein alpha-receptor activity, Clin. Pharmacol. Ther. 38 (1985) 495–502.

APPENDIX A

B = transmission channel bandwidth

P_N = noise power,

Source (skin, blood, fat) to destination

P_0 = transmission power, δ_{c0}= channel gain, T_0 = required transmission rate,

$$T_{sd} = B\log_2(1+\frac{P_{t0}\delta_{c0}}{L_{path}P_N})$$

$$L_{path} = (\frac{4\pi dn_m}{\lambda_0})^2 e^{\alpha(f)d}$$

$$T_{sd} = B\log_2(1+\frac{P_{t0}\delta_{c0}}{(\frac{4\pi dn_m}{\lambda_0})^2 e^{\alpha(f)d} * P_N})$$

Outage Probability, $P_{sd_{out}} = \Pr(T_{sd} \le T_0)$

$$= 1 - \Pr(T_{sd} \ge T_0)$$

$$=1 - \Pr(B\log_2(1+\frac{P_{t0}\delta_{c0}}{(\frac{4\pi dn_m}{\lambda_0})^2 e^{\alpha(f)d}*P_N})) \ge T_0$$

$$=1 - \Pr\left(\left(1+\frac{P_{t0}\delta_{c0}}{(\frac{4\pi dn_m}{\lambda_0})^2 e^{\alpha(f)d}*P_N}\right) \ge 2^{\frac{T_0}{B}}\right)$$

$$=1 - \Pr\left(\delta_{c0} \le \left(\left(\frac{\left(2^{\frac{T_0}{B}}-1\right)}{P_{t0}}\right) * P_N * L_{path}\right)\right)$$

$$=1 - \exp\left(-\left(\frac{\left(2^{\frac{T_0}{B}}-1\right)}{P_{t0}}\right) * P_N * L_{path}\right)$$

Source (skin, blood, fat) to Relay

P_{t1}= transmission power, δ_{c1}= channel gain, T_1= required transmission rate,

$$T_{sr} = B\log_2(1 + \frac{P_{t1}\delta_{c1}}{(\frac{4\pi dn_m}{\lambda_1})^2 e^{\alpha(f)d} * P_N})$$

Outage probability, $P_{sr_{out}} = \Pr(T_{sr} \leq T_1)$

$$= 1 - \Pr(T_{sr} \geq T_1)$$

$$=1 - \Pr(B\log_2(1 + \frac{P_{t1}\delta_{c1}}{(\frac{4\pi dn_m}{\lambda_1})^2 e^{\alpha(f)d} * P_N})) \geq T_1$$

$$=1 - \Pr\left(\left(1 + \frac{P_{t1}\delta_{c1}}{(\frac{4\pi dn_m}{\lambda_1})^2 e^{\alpha(f)d} * P_N}\right) \geq 2^{\frac{T_1}{B}}\right)$$

$$=1 - \Pr\left(\delta_{c1} \leq \left(\left(\frac{\left(2^{\frac{T_1}{B}} - 1\right)}{P_{t1}}\right) * P_N * L_{path}\right)\right)$$

$$=1 - \exp\left(-\left(\frac{\left(2^{\frac{T_1}{B}} - 1\right)}{P_{t1}}\right) * P_N * L_{path}\right))$$

Relay to destination

P_{t2}= transmission power, δ_{c2}= channel gain, T_2= required transmission rate,

$$T_{rd} = B\log_2(1 + \frac{P_{t2}\delta_{c2}}{L_{path}P_N})$$

Outage probability, $P_{rd_{out}} = \Pr(T_{rd} \leq T_2)$

$$= 1 - \Pr(T_{rd} \geq T_2)$$

$$=1-\Pr(B\log_2(1+\frac{P_{t2}\delta_{c2}}{L_{path}P_N}))\ \geq T_2$$

$$=1-\Pr\left(\left(1+\frac{P_{t1}\delta_{c1}}{L_{path}P_N}\right)\geq 2^{\frac{T_2}{B}}\right)$$

$$=1-\Pr\left(\delta_{c2}\leq\left(\left(\frac{\left(2^{\frac{T_2}{B}}-1\right)}{P_{t2}}\right)*P_N*L_{path}\right)\right)$$

$$=1-\exp\left(-\left(\frac{\left(2^{\frac{T_2}{B}}-1\right)}{P_{t2}}\right)*P_N*L_{path}\right)$$